CONTROL STRATEGIES FOR COMMUNICATION INDEPENDENT ISLANDING DETECTION IMPLEMENTATION

A DISSERTATION

SUBMITTED IN PARTIAL FULFILLMENT OF THE REQUIREMENTS
FOR THE AWARD OF THE DEGREE
OF

MASTER OF TECHNOLOGY
IN

POWER ELECTRONICS AND SYSTEMS

Submitted by:

SAMAVEDAM SWETHA

2K21/PES/17

Under the supervision of:

PROF. VISHAL VERMA
(Professor, EED, DTU)

DEPARTMENT OF ELECTRICAL ENGINEERING
DELHI TECHNOLOGICAL UNIVERSITY
(Formerly Delhi College of Engineering)
Bawana Road, Delhi – 110042

MAY, 2023

DELHI TECHNOLOGICAL UNIVERSITY

(Formerly Delhi College of Engineering)
Bawana Road, Delhi – 110042

CANDIDATE'S DECLARATION

I, **SAMAVEDAM SWETHA**, 2K21/PES/17, student of MTech (Power Electronics and Systems), hereby declare that the project Dissertation titled "CONTROL STRATEGIES FOR COMMUNICATION INDEPENDENT ISLANDING DETECTION IMPLEMENTATION" which is submitted by me to the Department of Electrical Engineering, Delhi Technological University, Delhi in partial fulfilment of the requirement for the award of the degree of Master of Technology, is original and not copied from any source without proper citation. This work has not previously formed the basis for the award of any Degree, Diploma Associateship, Fellowship or other similar title or recognition.

Place: Delhi **SAMAVEDAM SWETHA**

Date:

DEPARTMENT OF ELECTRICAL ENGINEERING

DELHI TECHNOLOGICAL UNIVERSITY

(Formerly Delhi College of Engineering)

Bawana Road, Delhi – 110042

CERTIFICATE

I hereby certify that the Project Dissertation titled "CONTROL STRATEGIES FOR COMMUNICATION INDEPENDENT ISLANDING DETECTION IMPLEMENTATION" which is submitted by **SAMAVEDAM SWETHA** , Roll No. 2K21/PES/17, Department of Electrical Engineering, Delhi Technological University, Delhi in partial fulfilment of the requirement for the award of the degree of Master of Technology, is a record of the project work carried out by the student under my supervision. To the best of my knowledge this work has not been submitted in part or full for any Degree to this University or elsewhere.

Place: Delhi

Date:

PROF. VISHAL VERMA

(SUPERVISOR)

ACKNOWLEDGEMENT

I would like to express my gratitude towards all the people who have contributed their precious time and effort to help me without whom it would not have been possible for me to understand and complete the project.

I would like to thank **Prof. Vishal Verma** (Professor, Department of Electrical Engineering, DTU, Delhi) my Project guide, for supporting, motivating, and encouraging me throughout the period of this work was carried out. His readiness for consultation always, his educative comments, his concern and assistance even with practical things have been invaluable. Besides my supervisor, I would like to thank all the PhD. scholars of Simulation Lab, for helping me wherever required and provided me continuous motivation during my research. Finally, I must express my very profound gratitude to my father, Dr. Sriman Samavedam Vijay Raghavan, my mother, Dr. Saripalli Vijaya Durga, my sister Dr. Samavedam Sravya, seniors and to my friends for providing me with unfailing support and continuous encouragement throughout the research work.

Date: 31.05.2023

SAMAVEDAM SWETHA
M.Tech Power Electronics and Systems
(2K21/PES/17)

ABSTRACT

This thesis project focuses on the investigation and integration of two islanding detection methods: the fuzzy inferencing system (FIS) and the wavelet packet transform (WPT). The primary objective is to address the limitations of the FIS method through the incorporation of the WPT method, while also ensuring independence from a communication system. The FIS method offers a robust framework for modelling complex relationships and uncertainties in power systems. However, it may exhibit limitations in accurately analysing transient events and disturbances, potentially leading to false detection outcomes. To overcome these limitations, the WPT method is introduced, which decomposes power system signals into frequency sub-bands, enabling the capture of unique patterns associated with islanding events.

Through extensive simulation experiments, the effectiveness of both the FIS and WPT approach are evaluated. The simulation results consistently support the superiority of the WPT method compared to the FIS method. Moreover, a significant advantage of the proposed methods is their independence from a communication system. This aspect eliminates the need for additional infrastructure and reduces the potential for communication failures or latency issues that can affect the reliability of the islanding detection process.

The findings of this thesis project have important practical implications. The research outcomes contribute to the development of advanced protection mechanisms that enhance the resilience and stability of power systems, catering to the needs of the increasing DG penetration into the grid. Looking ahead, the future scope of this research includes further optimization of the combined FIS and WPT method, integration with advanced machine learning techniques, real-time implementation, testing in diverse power system scenarios, validation against alternative islanding detection methods, and integration with smart grid technologies.

TABLE OF CONTENTS

LIST OF FIGURES

LIST OF TABLES

LIST OF ABBREVIATIONS

DG	Distributed/Decentralized generation
μG	Microgrid
PCC	Point of Common Coupling
V_{pcc}	Voltage at point of common coupling
ANN	Artificial Neural Network
PNN	Probabilistic Neural Network
SVM	Support Vector Machine
FL	Fuzzy Logic
FIS	Fuzzy Inferencing System
WPT	Wavelet Packet Transform
DFT	Discrete Fourier Transform
FFT	Fast Fourier Transform
DWT	Discrete Wavelet Transform
WPD	Wavelet Packet Decomposition
IDM	Intelligent Detection Method

CHAPTER 1

INTRODUCTION

1.1 EMBRACING SUSTAINABLE POWER GENERATION

The urgency to harness renewable energy sources stems from several compelling factors. Firstly, mitigating climate change has become a pressing imperative. Fossil fuel combustion significantly contributes to global warming, making the transition to renewables a viable solution. By reducing greenhouse gas emissions, renewable energy plays a crucial role in slowing climate change. Secondly, ensuring energy security is critical. Dependence on fossil fuels from limited and geopolitically volatile regions poses risks to stability. Embracing renewable energy sources allows countries to diversify their energy mix and reduce dependence on imported fossil fuels. This enhances energy security and decreases vulnerability to supply disruptions, ensuring a more stable and reliable energy supply.

Moreover, the environmental benefits of renewables cannot be overstated. Traditional energy sources cause severe environmental damage, including pollution and habitat destruction. Renewable energy sources have lower environmental footprints, enabling the protection of ecosystems, preservation of biodiversity, and mitigation of environmental harm. Transitioning to renewables reduces air pollution, improving air quality and reducing respiratory and cardiovascular diseases. Additionally, harnessing renewable energy offers substantial economic opportunities. The renewable energy sector generates jobs, attracts investment, and drives technological innovation. Investing in renewable energy infrastructure stimulates economic growth, enhances energy affordability, and fosters local development, particularly in underserved areas.

Energy access and equity are also crucial considerations. Many regions still lack reliable electricity access, which renewable energy can address. Technological advancements and cost reductions have made renewables increasingly viable and competitive. Improvements in efficiency and affordability have enhanced the feasibility of harnessing renewable energy sources for power generation.

Furthermore, policy and international commitments play a significant role. Governments and international bodies recognize the importance of transitioning to renewables for sustainable development and addressing climate change. Numerous nations have established objectives for renewable energy, enacted favourable policies, and provide incentives to promote its adoption, demonstrating a worldwide agreement regarding the necessity of renewable energy.

1.2 COMPREHENDING THE MASTER – SLAVE CONFIGURATION

Taking into consideration the above pressing reasons, shift towards renewable energy generation is adopted. These newer forms of power generation rely on power electronic interfaces for efficient operation. As an example, the utilization of DC to AC inverters is vital for photo-voltaic arrays and fuel cells, whereas AC to DC to AC conversion becomes essential for variable speed wind turbines and high-speed gas turbine generators. Previously, the power generated could be utilized to power local loads, but owing to advancement of power electronic converters, power can now be harvested efficiently from the renewable sources, such that excessive power can now be injected into the grid for revenue generation. Distributed/Decentralized generation (DG) is a classification that encompasses connected loads, storage systems, and control strategies to integrate renewable energy sources (RES). These systems, commonly referred to as μG, could function in both grid-tie mode and islanded mode [1].

Integrating DG sources with the microgrid requires careful control, especially considering the unique characteristics of inverters compared to conventional electrical machines. Inverters offer a wide bandwidth and enable control over power export and waveform quality. Effective control is necessary due to the limited short-time overload ratings of inverters and the importance of load sharing. Moreover, inverters commonly incorporate an inductive filter that effectively hinders current emissions at the switching frequency by offering a substantial impedance. However, it is possible that this filter will still exhibit a relatively high impedance when it comes to low-order harmonic distortion. As a result, voltage distortion can occur across the filter due to harmonic currents generated by non-linear loads, thereby impacting neighbouring loads.

In contrast, traditional electrical machines, such as generators, possess different characteristics. The power export of these systems is regulated within a moderate bandwidth, and the waveform quality is predetermined during the design phase

by configuring the windings. These machines employ a low impedance source to guarantee the supply of fault current for fault clearance and to prevent significant voltage drops caused by harmonic currents. When DG supply power to a large and robust grid, the power export of small DGs can be adjusted as needed. However, during islanding situations, when physical isolation or desynchronization happens as a result of grid problems, it becomes essential to ensure compatibility between load and supply and establish a mechanism for distributing the load among generating units. In conventional electrical machines, load matching and sharing are achieved by employing governors or control settings that incorporate a specific frequency droop based on real power supply and a voltage droop considering reactive power. In the case of inverter-based systems, from a control perspective, it is advantageous to distribute reference signals to all inverters to guarantee the intended power matching and sharing. Several approaches have been suggested for the parallel operation of inverters in applications like UPS and photovoltaic power supply systems. Proximity between inverters enables the utilization of methods like central mode, distributed logic mode and master-slave mode to facilitate the communication of control signals among them [2].

In a microgrid, master-slave operation control strategy is used to coordinate and manage multiple inverters that are connected to the microgrid. In this setup, one inverter acts as the master and takes the lead in controlling and regulating the power flow within the microgrid. The other inverters, known as slaves, follow the instructions provided by the master inverter. In the context of control functions, the terms "master" and "slave" are used to distinguish the roles assigned to different inverters within a group. From a technological standpoint, all the inverters are identical. However, due to physical proximity and their connection to a shared node, it is not feasible for all inverters to independently control the output voltage. Instead, a specific inverter is assigned the role of the master, assuming responsibility for regulating the voltage at the node. It is worth noting that this role can be assigned to different inverters at different times, as needed. The remaining inverters within the group function as slaves, collectively supplying current to the common node to share the power generation. Thus, the master inverter determines the reference signals, such as voltage and frequency, and communicates them to the slave inverters to achieve power sharing, load balancing, and overall system coordination [3]. By employing this control arrangement, all inverters are synchronized and collaborate to uphold the stability and dependability of the microgrid. This arrangement helps optimize the performance and efficiency of the microgrid by

effectively managing the DG sources and maintaining grid stability. In the event of an islanding situation, when the master DG unit becomes disconnected from the rest of the system, one of the remaining slave DGs needs to transition into the role of the master and ensure voltage balance, while the remaining slave DGs support to strike load balance by injecting current. Thus, it becomes vital to detect condition of islanding.

1.3 REQUISITE FOR ISLANDING DETECTION

Islanding is defined as "A condition in which a portion of the utility system that contains both load and distributed resources remains energized while isolated from the remainder of the utility system. [4] " This isolation usually arises from disruptions within the electric utility network, like malfunctions or notable variations in frequency and/or voltage resulting from imbalances between real and reactive power. Two options arise in such situations: Firstly, the decision to maintain the DG connected to the system and continue supplying power to the load, based on the criticality and requirements of the load. Secondly, the alternative is to disconnect the DG from the system before the automatic reclosing time of the utility breaker elapses. If there is no synchronism check in place and the DGs fail to disconnect quickly, the utility breaker may attempt to reclose without synchronization. This imposes multiple operational constraints such as voltage instability, transients, and power quality disturbances, etc., which can affect the reliability and efficiency of the µG adhering to the existing standards such as IEEE 1547 – 2018 [5], UL 1741 [6], and IEC – 62116 shown in TABLE 1.1. Thus arises the need for precise, prompt, and cost-effective detection of islanding conditions [7].

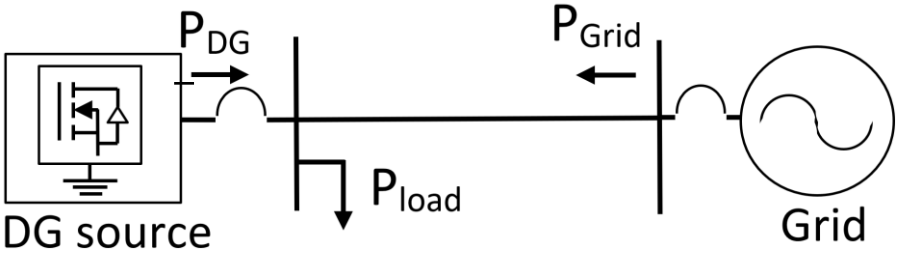

Fig 1.1 Single line diagram of a small part of the µG before islanding

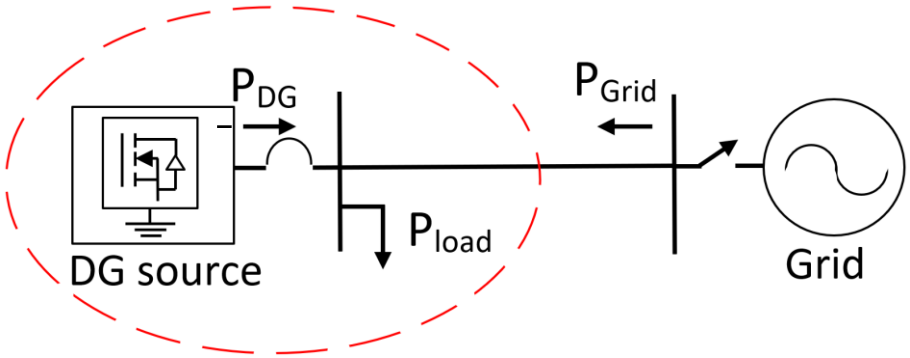

Fig 1.2 Single line diagram of a small part of the μG in case of islanding condition

TABLE 1.1 STANDARDS FOR ISLANDING DETECTION

Parameters	IEEE Std. 1547-2003	IEEE Std. 929-2000	IEC 62116	Korean Standard
Quality factor	1	2.5	1	1
Detection time	t < 2s	t < 2s	t < 2s	t < 0.5s
Allowed Frequency Range (nominal frequency f_o)	59.3 Hz ≤ f ≤ 60.5 Hz	59.3 Hz ≤ f ≤ 60.5 Hz	f_o – 1.5 Hz ≤ f and f ≤ (f_o + 1.5 Hz)	59.3 Hz ≤ f ≤ 60.5 Hz
Allowed Voltage Range (nominal voltage V_o)	0.88 ≤ V ≤ 1.10	0.88 ≤ V ≤ 1.10	0.85 ≤ V ≤ 1.15	0.88 ≤ V ≤ 1.10

1.4 Objectives of the thesis work

The goals of this thesis work are :

- To emphasise the need to shift towards cleaner energy generation and utilise them to their full potential.
- To gain a comprehensive understanding of the key aspects involved in harnessing cleaner energy sources for commercial purposes and to subsequently develop appropriate control strategies based on this understanding.
- To develop a thorough comprehension of various islanding detection methodologies that currently exist in the literature and identify the research gap by drawing insightful conclusions. Additionally, this research aims to address these gaps by introducing two novel methods for islanding detection, each addressing the limitations of the other.
- To understand Goertzel Algorithm, Fuzzy Logic Controller, and WPT through islanding detection perspective.

1.5 Organization of the thesis work

As previously stated, the primary aim of this thesis is to develop an islanding detection methodology that is resilient, efficient, and capable of delivering accurate and rapid results. Furthermore, the proposed methodology should be independent of communication systems, ensuring its reliability and applicability in various scenarios. The thesis is organized as follows to achieve this goal:

Chapter 1 This chapter offers an introduction to the renewable energy scenario, as well as a concise overview of the control strategy employed by multiple parallel inverters and the existing literature on islanding detection methods.

Chapter 2 By following this organization, the thesis aims to deliver a comprehensive and insightful analysis of the proposed islanding detection methodologies, their performance, and their potential impact on power system operation.

Chapter 3 This chapter provides with a deeper understanding with the mathematical background of Goertzel algorithm and wavelet packet transform to help better understand the following chapters, Chapter 4 and Chapter 5.

Chapter 4 This chapter provides complete understanding of proposed islanding detection method that utilizes Goertzel algorithm in collaboration with Fuzzy inferencing system. This proposed method is independent of communication system requirement.

Chapter 5 This chapter discusses in detail the implementation Wavelet Packet transformation method for islanding detection, with the the motive to address the gap caused due to FIS based islanding detection technique. The proposed method is supported with simulation results to prove the same.

Chapter 6 This chapter provides a detailed conclusion of the various islanding detection methods, and also discusses the future scope of this work.

CHAPTER 2

LITERATURE REVIEW

2.1 BACKGROUND

Different IDMs have been suggested in research literature wherein each method possesses its unique strengths and weaknesses concerning the Non-detection zone (NDZ), reactive power, and detection time. These islanding detection methods can be categorized into remote schemes, local schemes, and intelligent classifier-based schemes, as illustrated in the accompanying Fig 2.1.

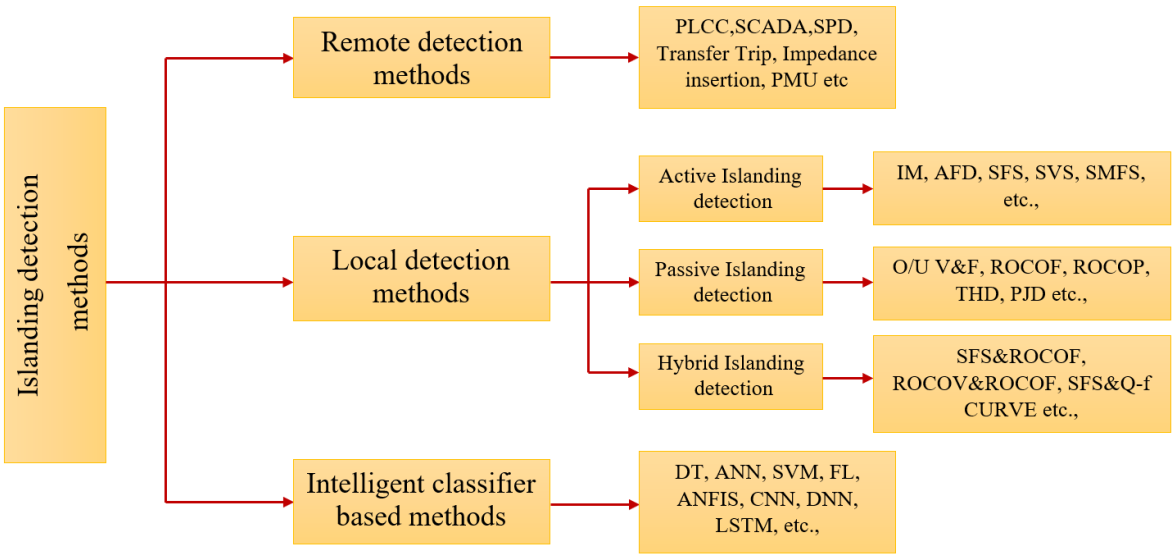

Fig 2.1 Classification of IDMs

Remote islanding detection methodology refers to the approach used to identify islanding conditions in a power system remotely. It entails observing different factors and signals to establish whether a section of the power system has been electrically disconnected from the primary utility grid. Establishing a communication link between the DG and the main utility necessitates the use of supplementary equipment, such as costly sensors, telecommunication tools, and control systems [9], [10], [11]. Remote islanding detection systems generally entail higher initial and operational expenses when compared to active and passive techniques. As a result, they

are more commonly used in large-scale projects rather than small-scale systems [12]. However, remote islanding detection systems offer several advantages such as no non-detection zone, no degradation of power quality, and the ability to handle complex DG integrated power systems. Remote islanding detection systems comprise various examples such as power line carrier communication (PLCC) [13], [14], [15], supervisory control and data acquisition (SCADA) [10], [16], [17] signals produced disconnect (SPD) [18], [19], [20], transfer trip schemes (TPS) [21], [22], [23], impedance insertion method [21], and phasor measurement unit (PMU) [24 - 29].

Local schemes for islanding detection depend on the monitoring of electrical parameters, including voltage, current, frequency, and power. Additionally, these schemes involve introducing disturbances into the distributed generation-enabled power system (DG-EPS) to detect islanding. Islanding detection methods (IDMs) are classified into active, passive, and hybrid schemes. Active IDMs involve the injection of external disturbances into the DG output, causing variations in system parameters [30,31].By comparing these variations against predefined thresholds, active methods can detect islanding. Active IDMs present benefits such as a reduced NDZ and quicker detection time. However, they necessitate additional configuration for disturbance injection, which can potentially impact the power quality of the distributed generation-based electrical power system (DG-EPS). The literature presents various active IDMs, including impedance measurement (IM) [32-34], active frequency drift (AFD) [35-38], Sandia frequency shift (SFS) [40-42], Sandia voltage shift (SVS) [43-45], and sliding mode frequency shift (SMFS) [46-49].

Passive islanding detection is another widely employed method in the context of distributed generation-enabled power systems (DG-EPS). In this approach, The system parameters are continuously monitored at the point of common coupling (PCC) to detect any changes that may indicate the isolation of the utility system from the DG-EPS [50-52]. By comparing these variations against predefined threshold values [53-54], the protective relay can detect islanding. Passive islanding detection schemes are cost-effective and straightforward, posing no negative impact on power quality, making them practical solutions for DG-EPS. However, passive IDSs have a larger non-detection zone (NDZ) and require the establishment of threshold value [55-57]. Examples of passive IDMs found in the literature include over/under voltage and frequency methods (O/U V&F) [58-61], rate of change of frequency/power (ROCOF/P)

[64-66], total harmonic distortion method (THD) [67-70], and phase jump detection (PJD) methods [71-73].

Hybrid islanding detection methods (HIDMs) combine the advantages of both active and passive schemes to address the limitations of each. By employing hybrid IDMs, it is possible to mitigate the power quality issues associated with active IDSs and overcome the larger non-detection zone (NDZ) of passive IDSs [74,75]. However, hybrid IDMs tend to be more complex and may have longer detection times. The literature presents several hybrid schemes for islanding detection, such as those incorporating positive feedback and voltage unbalance, Sandia frequency shift (SFS) and rate of change of frequency (ROCOF), voltage unbalance and frequency set point, voltage and real power shift, ROCOV and ROCOP, as well as hybrid SFS and Q-f Curve IDMs. These hybrid approaches offer a potential solution to enhance the effectiveness of islanding detection in distributed generation-enabled power systems [75-80].

IDMs based on remote and local schemes come with their own set of pros and cons [81-84]. Remote schemes, while reliable for large systems, require a communication interface and can be impractical for smaller systems due to their complexity and higher cost [85,86]. In contrast, local schemes are known for their simplicity, ease of implementation, and cost-effectiveness. However, they are not without their drawbacks. Active methods employed in local schemes may suffer from noise and power quality issues, while passive islanding schemes often have a large NDZ and lower detection speed [88,89]. Recognizing the limitations of both local and remote schemes, there is a growing interest in intelligent classifier-based schemes for islanding detection. These intelligent schemes eliminate the need for threshold settings, address noise and power quality problems, offer a lower NDZ, faster detection speed, and do not require intervention from a communication channel. Consequently, intelligent classifier-based schemes are gaining recognition as more reliable and viable alternatives in islanding detection. A brief understanding of intelligent IDM's is presented in the next section.

2.2 INTELLIGENT IDMs

Intelligent IDMs share similarities with communication- or signal processing-based approaches, yet they have the advantage of eliminating the need for threshold selection. These methods leverage various intelligent classifiers and data mining techniques to effectively detect islanding events. Commonly used in intelligent

islanding detection are signal processing techniques like Artificial Neural Networks (ANN), Decision Tree (DT), Probabilistic Neural Networks (PNN), Support Vector Machines (SVM), and Fuzzy Logic (FL).These techniques excel at addressing multi-objective problems that conventional approaches may struggle to handle. Figure 2.2 illustrates a diagram showcasing intelligent islanding detection methods. Initially, the input signal, which can be voltage or current measured at the point of common coupling (PCC), is employed in the first phase for data training and feature extraction through a training algorithm. This offline procedure saves time and reduces computational load. In the next step, the online process applies an intelligent classifier model to reach the final decision. The following subsections provide a concise overview of intelligent islanding detection methods.

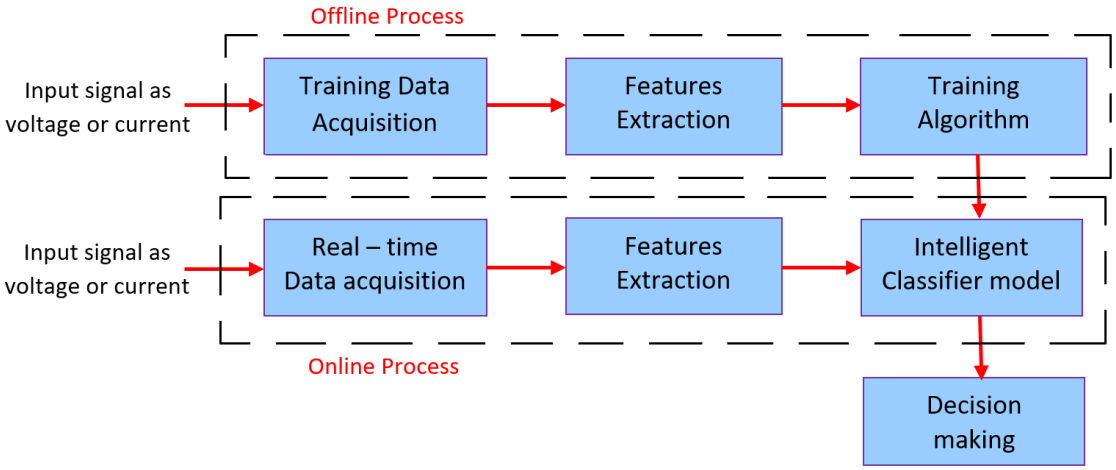

Fig 2.2 Understanding functionality of intelligent IDMs

2.2.1 Artificial Neural Network (ANN) based method

ANN-based methods utilize measuring data to extract significant features that aid in detecting variations in power system parameters. ANN, a computational model inspired by biological processes, mimics the neural network of the human brain, and incorporates valuable information and data memory [90]. These ANN-based islanding detection methods offer precision and effective operation for systems with multiple inverter [91]. However, they still face challenges related to extensive processing time and feature selection, particularly when dealing with various configurations of DG. Resolving these issues is crucial for further enhancing the efficiency of ANN-based schemes in islanding detection.

2.2.2 Decision Tree – based method

In the field of signal processing and intelligent islanding detection methods (IDMs), decision tree (DT) classifiers are commonly used in combination with wavelet packet transform (WPT) or discrete wavelet transform (DWT) [92]. The voltage or current signals acquired from the terminals of DG are typically subjected to WPT or DWT to extract relevant features. The extracted features are subsequently examined by a DT classifier to ascertain the occurrence of islanding.

2.2.3 Probabilistic Neural Network (PNN) based method

The PNN functions as a classification method that can calculate non-linear decision boundaries using a Bayesian classifier. It is widely employed in traditional pattern recognition systems that utilize artificial neural hardware. It comprises four layers: the input layer, pattern layer, summation layer, and output layer. Each layer serves a distinct role in feature classification without the requirement of any learning technique. The favourable characteristics of PNN-based methods establish them as a reliable option for islanding detection. [93]

2.2.4 Support Vector Machine (SVM) – based method

The SVM is a dependable classification technique used in the analysis of signals and systems. It establishes a decision boundary to differentiate the training data. By incorporating autoregressive modelling, the SVM classifier effectively captures unique characteristics from voltage or current signals measured at the PCC. SVM-based intelligent islanding detection methods provide correctness and fast detection speed. Nevertheless, the computational load linked to data training and the intricate nature of the algorithm make SVM-based intelligent islanding detection methods unfeasible for practical implementation in real-world systems. [94-95]

2.2.5 Fuzzy – logic (FL) based method

FL techniques are applied as a classifier approach based on fuzzy rules to detect islanding. FL, initially introduced alongside DT transformation, integrates fuzzy membership functions and rule-based formulations to augment fuzzy systems. When utilized in islanding detection algorithms, these methods exhibit effective performance. Nonetheless, fuzzy classifiers have limitations due to the high abstraction resulting from the multitude of combinations of maximum and minimum classes. Moreover, FL-based approaches are susceptible to being sensitive to noisy data because of the iterative generation of membership function rules and classifications.

2.3 RESEARCH GAP AND MOTIVATION

Based on the insights gained from the preceding sections, an ideal islanding detection method should possess several characteristics, including promptness, cost-effectiveness, independence from communication systems, and freedom from errors. This thesis presents two distinct approaches for islanding detection, with the latter approach addressing the limitations of the former.

The first method proposed for islanding detection involves the application of the Goertzel algorithm in collaboration with a fuzzy logic controller. This methodology ensures prompt and accurate detection of islanding events while adhering to established standards. However, a drawback of this approach is the occurrence of noise amplification resulting from the repeated generation of membership functions and rules.

To overcome this limitation, an improved islanding detection methodology is introduced, which is based on the wavelet packet transform. This enhanced approach offers a solution to the problem of noise amplification by utilizing wavelet packet analysis. By employing this technique, the detection accuracy can be improved while mitigating the negative effects of noise.

CHAPTER 3

BACKGROUND AND CONTEXTUAL FRAMEWORK

3.1 MATHEMATICAL BACKGROUND OF GOERTZEL ALGORITHM

The Goertzel algorithm is an optimized variant of the discrete Fourier transform, taking a convolutional approach to enhance its efficiency, computes the Fourier value at a specific frequency position, making it ideal for evaluating selected bins in the Fourier spectrum. The versatile characteristics allow for its utilization as a digital filter as well. The fundamental relationship of the discrete Fourier transform, represented by Equation (3.1), can be transformed into a convolutional form, as depicted in Equation (3.2). In this form, x(p) denotes the p^{th} sample of the signal in the time domain, while X(q) represents the q^{th} bin of the Fourier spectrum. The rectangular weighing function u(l) is used in this context.

$$X(q) = \sum_{p=0}^{N-1} x(p).e^{-j2\Pi p\frac{q}{N}} \tag{3.1}$$

$$\begin{aligned} y_q(l) &= \sum_{r=-\infty}^{\infty} x(p).e^{j2\Pi(N-p)\frac{q}{N}}.u(l-p) \\ &= x(p).e^{j2\Pi l\frac{q}{N}}|_{l=N} \end{aligned} \tag{3.2}$$

The derived filter exhibits an impulse response, as illustrated in Equation (3.3), which takes the form of a complex harmonic signal. The length of this signal is limited by a rectangular window.

$$h(l) = e^{j2\Pi l\frac{q}{N}} \tag{3.3}$$

By utilizing the Z-transform on the impulse response, as defined in Equation (3.3), it enables the computation of the transfer function of the Goertzel filter, represented in Equation (3.4). For ease of implementation, the modified form of the

Goertzel algorithm, depicted in Equation (3.5), is more practical. The modified form can be split into two components: the real recursive component and the complex direct computational component.[96]

$$H(z) = \sum_{l=0}^{\infty} h(l).z^{-1} = \frac{1}{1 - z^{-1}.e^{j2\Pi\frac{q}{N}}} \tag{3.4}$$

$$H(z) = \frac{1}{1 - z^{-1}.e^{j2\Pi\frac{q}{N}}} . \frac{1 - z^{-1}.e^{-j2\Pi\frac{q}{N}}}{1 - z^{-1}.e^{-j2\Pi\frac{q}{N}}}$$

$$= \frac{1 - z^{-1}.e^{-j2\Pi\frac{q}{N}}}{1 - 2z^{-1}\cos\left(2\Pi\frac{q}{N}\right) + z^{-2}} \tag{3.5}$$

Fig 3.1 illustrates the implementation of the transfer function depicted in Equation (3.5). It is crucial to emphasize that the filter possesses two complex poles that are precisely positioned on the unit circle, guaranteeing stability. Consequently, the loop can generate an impulse response with a consistent amplitude. However, if there is any uncertainty in the coefficient C, such as due to quantization errors, it can lead to a fading effect in the impulse response. This effect becomes more pronounced, particularly when dealing with large coefficients for both q and N.

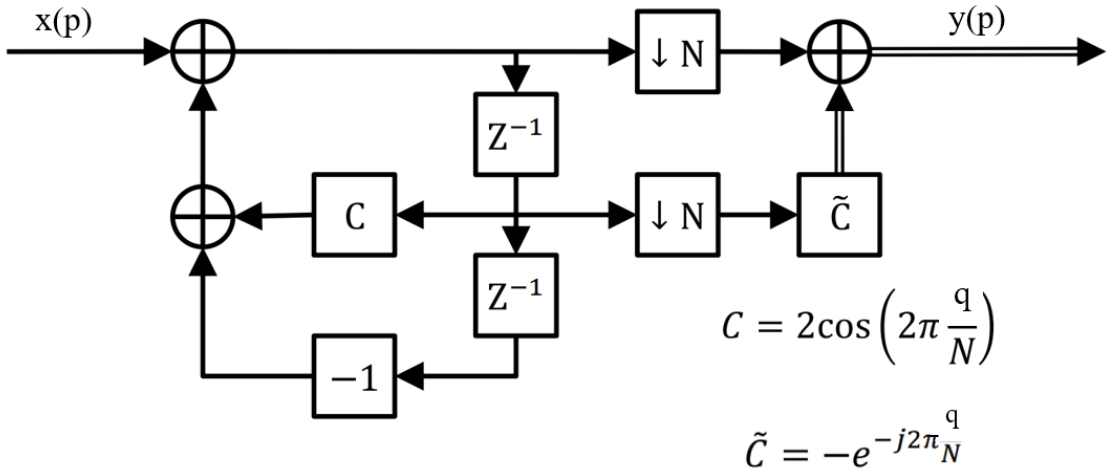

Fig 3.1 Signal diagram of Goertzel filter

The down-sampling blocks satisfy the condition specified in Equation (3.2) and successfully apply the rectangular windowing technique to the impulse response. The direct part of the algorithm is responsible for evaluating the complex output.

3.1.1 Transfer function of Goertzel filter

The literature lacks extensive discussion on the derivation of filtration characteristics. Due to the limitation imposed by N samples before the filter is reset, substituting $e^{j\omega}$ into the derived transfer function (Equation 3.4) does not yield the power spectral density. To obtain the accurate frequency characteristics, the impulse response from Equation (3.3) is subjected to the inverse Fourier transform, which can be easily reproduced in Equation (3.6).

$$\begin{aligned} H_{Goertzel}(f) &= \int_{-\infty}^{\infty} u(l-p).e^{j2\Pi l\frac{q}{N}}.e^{j2\Pi fl}dl \\ &= \frac{1}{N}\int_{0}^{N} e^{j2\Pi l\frac{q}{N}}.e^{j2\Pi fl}.dl \end{aligned} \tag{3.6}$$

After performing certain calculations, the result is the complex spectrum as depicted in Equation (3.7). The filter's power spectral density is depicted in the Equation (3.8), while Equation (3.9) represents the phase characteristic.

$$\begin{aligned} H_{Goertzel}(f) &= \frac{e^{j2\Pi\left(\frac{q}{N}-f\right)N}-1}{j2\Pi\left(\frac{q}{N}-f\right)N} \\ &= \frac{\sin\left(\Pi q-\Pi fN\right)}{\Pi q-\Pi fN}e^{j\Pi\left(\frac{q}{N}-f\right)N} \end{aligned} \tag{3.7}$$

$$|H_{Goertzel}(f)|^2 = \frac{\sin\left(\Pi q-\Pi fN\right)^2}{\Pi^2(q-fN)^2} \tag{3.8}$$

$$arg\left(H_{Goertzel}(f)\right) = \Pi\left(\frac{q}{N}-f\right)N \tag{3.9}$$

Unlike the DFT or its fast implementation, the FFT, which typically restricts adjustments to integer frequencies, this filter allows for fine-tuning to non-integer frequencies. In contrast, when employing the DFT, the frequency remains fixed for each bin and is exclusively influenced by the duration of the DFT, denoted as N. However, the Goertzel algorithm conveniently allows for the use of any real frequency within the sampled range without encountering any issues.

3.2 UNDERSTANDING WAVELET PACKET TRANSFORM

3.2.1 Discrete Wavelet Transform (DWT)

The wavelet transform demonstrates multi-resolution analysis properties, allowing it to capture local signal characteristics in both temporal and spectral domains. This method conducts multiscale analysis by employing expansion and translation

calculation functions. Unlike the Fourier transform, the wavelet transform provides a time-frequency window that dynamically adjusts with frequency, effectively highlighting specific aspects of the signals. Out of numerous wavelet transforms, the DWT stands as the fundamental and extensively utilized one. It employs a two-channel filter bank at multiple levels for implementation. Through discretizing the scale and displacement of the continuous wavelet transform using powers of 2, the DWT is commonly referred to as the dyadic wavelet transform. [97]

During the process of DWT decomposition, the low-frequency component, which captures the characteristics of the signal at higher scales, serving as an approximation that often encompasses its fundamental attributes. On the other hand, the high-frequency component reveals signal details or differences. Through a series of continuous decomposition steps using two mutually related filters, the original signal generates two signals. The approximation signal undergoes continuous decomposition, resulting in multiple low-resolution components. Theoretically, the decomposition process can continue indefinitely. In real-world applications, the decision regarding the number of decomposition layers is typically grounded on signal characteristics or predefined criteria. [97].

Rather than directly computing the scalar product between signals and the wavelet function $\psi(t)$ or the scaling function $\varphi(t)$, the DWT employs high-pass filter r[n] and low-pass filter s[n] to process the signal. By treating the wavelet coefficients $c_j[l]$ and $d_j[l]$ as discrete signals and r[n] and s[n] as digital filters, the DWT and filter bank are established. This approach is rooted in the fundamental principles of filter bank theory, which establishes the link between signal analysis and wavelet analysis. Wavelet analysis is commonly incorporated in the design of filter banks in various research studies. In the DWT, a down-sampling filter is applied following the low-pass and high-pass filters. Considering the original signal x[m], computation of j^{th} level components is as follows:

$$x_{i,r}[n] = \sum_{l=0}^{L-1} x_{i-1,r}[2n-l]r[l] \tag{3.10}$$

$$x_{i,s}[n] = \sum_{l=0}^{L-1} x_{i-1,s}[2n-l]s[l] \tag{3.11}$$

Here, L represents the length of the filters, while r[n] and s[n] denote the high-pass and low-pass filters, respectively.

3.2.2 Extension to DWT – Wavelet Packet Transform (WPT)

The wavelet packet method expands upon wavelet decomposition, providing a wider range of options for signal analysis and allowing the selection of the most appropriate analysis for a given signal. It facilitates a systematic conversion of a signal from the temporal domain to the spectral domain, offering enhanced flexibility in the analysis process. During this transformation, recursive filter-decimation operations are performed, resulting in a balancing act between time resolution, which decreases, and frequency resolution, which increases.

Unlike the wavelet transform, which divides the signal into unequal-width frequency bins, the wavelet packet method divides both the low and high frequency sub-bands, resulting in equally sized frequency bins. In wavelet analysis, the signal undergoes an initial partitioning into an approximation coefficient and a detail coefficient. The approximation coefficient is then further subdivided into second-level approximation coefficients and detail coefficients, with this persistive iterative process. Wavelet packet analysis expands on wavelet analysis by allowing both the approximation and detail components to be further split, resulting in multiple ways to encode the signal. Unlike the wavelet transform, which allows only the lowpass filter output to undergo further filtering iterations, the wavelet packet transform (WPT) permits iteration of both the lowpass and high pass filter outputs. This iterative capability of the high pass filter outputs in the WPT introduces the possibility of having multiple basis functions (or wavelet packets) at a given scale.

The collection of wavelet packets encompasses the complete family of potential bases, offering a wide range of basic functions. The wavelet basis is obtained when iterating only the low-pass filter, while the fully iterated wavelet packet tree results in the complete tree basis. The uppermost level of the wavelet packet decomposition (WPD) tree represents the signal in the time domain. While progressing through each level of the tree, there exists a give and take relationship between time and frequency resolution, with a greater emphasis on frequency resolution. The final level of complete tree decomposition provides the signal's frequency representation at its lowest level. Fig 3.2 illustrates the wavelet decomposition tree of both the DWT and WPT.

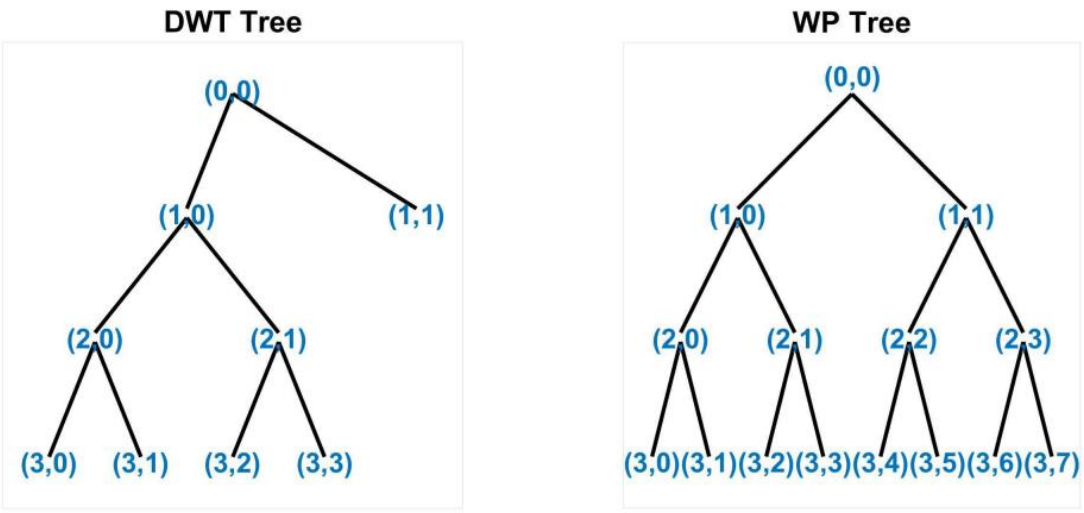

Fig 3.2 Wavelet decomposition tree: a) DWT tree, b) WPT tree

3.3 SYSTEM UNDER STUDY

For the analysis and control design in this thesis work, a basic μG structure is depicted in Fig 3.3. The μG consists of three Distributed Generators (DGs) connected to the system, specifically Photovoltaic-fed Inverters. Each DG has a maximum power rating of 4kW. At each feeder, there are three local loads connected, and each DG is linked to the 415V grid in a transformer-less configuration. Furthermore, the DGs operate in current control mode and inject power at unity power factor with respect to their Point of Common Coupling (POCC). The main utility grid is represented by a 415V, 50Hz AC source with a series line impedances (lumped) Z_1 and Z_2. To analyse the dynamics and evaluate the effectiveness of the proposed islanding detection method, the following assumptions are considered:

- The microgrid shows the competence to operate in both grid-connected mode and islanded mode, facilitated using a circuit breaker (CB) in conjunction with the utility grid.
- Between two sources, resistive line impedance is considered, being a distribution line operating at low voltage levels.
- Due to the low line reactance, the V_{pcc} of each DG is expected to be nearly in phase with each other. Therefore, the angle between the voltages is assumed to be infinitesimal.
- In the analysis, the assumption is made that the feeder exhibits a radial configuration, where the utility grid is connected at one end and the DGs are connected in a radial fashion.

- Each DG possesses knowledge of the number of DGs on both of its ends, as well as the end where the utility grid is connected.
- For the analysis and evaluation of the proposed algorithm, a system consisting of three DGs and a utility grid is considered.
- The line's distributed impedance is presumed by a lumped value, predominantly resistive in nature.

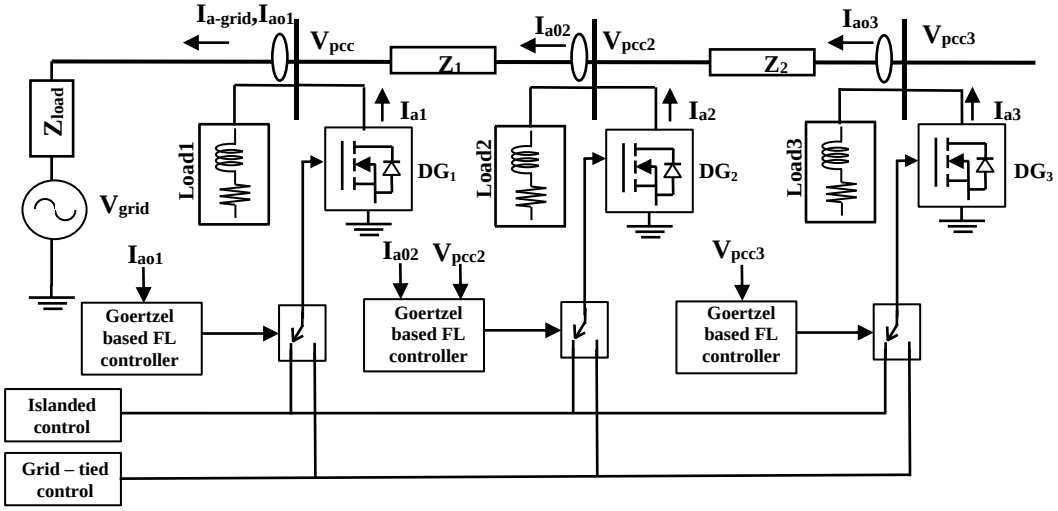

Fig 3.3 Microgrid structure employed for the islanding detection method proposed in the following two chapters

CHAPTER 4

ISLANDING DETECTION USING GOERTZEL ALGORITHM IN COLLABORATION WITH FUZZY INFERENCING SYSTEM

4.1 PROPOSED METHODOLOGY

This chapter suggests a reliable, effective, and quick islanding detection with DG tagging strategy for operation with multiple DGs in a μG system, by injecting ninth harmonic pilots, that can quickly identify grid islanding along with specific DGs failure. The Goertzel algorithm is employed at each node in autonomous mode to observe the 9^{th} harmonic component of the voltage at the point of common coupling (V_{pcc}) together with the current in the line around each node including the one transacting power with the grid interface. The injected balanced 9^{th} harmonic currents at a set value, aggregate vectorially at grid interfaced node to zero value, being equi - displaced phase, with respect to one another, thus causing extremely minimal harmonics impact, as they are injected into the grid by each DG. The 9^{th} harmonic detection by Goertzel algorithm is analysed using the Fuzzy logic at each DG node to enable the autonomous monitoring and control of the DG's connected to the μG.

4.2 PROPOSED ISLANDING DETECTION TECHNIQUE

Fig 3.3 depicts the single line diagram of the considered scaled down Microgrid structure employed for analysis and inferencing design in this work. Three DGs (Photovoltaic fed Inverters) are connected to the μG, where each DGs maximum power rating is kept at 3kW and is tied to the 415V distribution grid, injecting power at unity power factor through its PCC in GSM. The three local loads, each 4kW are connected at each PCC nodes. An AC source of 415V, 50Hz, and lumped line impedances Z_1 and Z_2 are represented for the modelling of the utility distribution grid to explore the efficiency of the proposed algorithm and to evaluate the suggested islanding detection approach. The line impedance between two sources is considered resistive, being a distribution line operating at low voltage levels. Owing to minimal line reactance, the V_{pcc} of each DG will be approximately in same phase with the other

accordingly, the angle between the V_{pcc} at line frequency is neglected. Accordingly, each DG is reprogrammed for updating the number of other DGs connected to the μG.

4.2.1 Harmonic component injection

The considered system is 3 - phase 4 – wired. Thus, the third harmonic and its odd multiple currents flow through the neutral wire, and do not flow in the line in balanced conditions. So, harmonic pilots of the order 3n, where n = 1,3,5,7,9…. can be injected in the line, to facilitate the islanding detection. Thus, phase-displaced 9^{th} harmonic current components of equal magnitude accounting to a Total Harmonic Distortion (THD) less than 4% as given in Table 4.1, are injected by each of the three DGs accounting to negligible grid current pollution. Accordingly, the angle between the current injected by the three DGs at 9^{th} harmonic will be 120˚ (360˚/n) where n is equal to 3. The following discussion will focus on single phase current and voltage phasors, with the extrapolation to the other two phases on similar logic. Thus, the current injected at the 9^{th} harmonic by DG nearer to grid connection, i.e., DG_1 will be at 0˚, whereas for the DG_2, it is kept at 240˚ and for DG_3 at 120˚ as shown in Fig 4.1. The total of the three harmonic current phasors, at 9^{th} harmonic adds to 0, thus the net harmonic current (at 9^{th} harmonic) injected into the grid would be zero eliminating the problem of grid pollution in active islanding detection methods as against others reported in the literature.

TABLE 4.1
MAXIMUM ALLOWED THD DUE TO HARMONIC CURRENT INJECTION

Harmonics	THD limit
3rd ~ 9th	< 4.0%
11th ~ 15th	< 2.0%
17th ~ 21st	< 1.5%
23rd ~ 33rd	< 0.6%
Above 33rd	< 0.3%

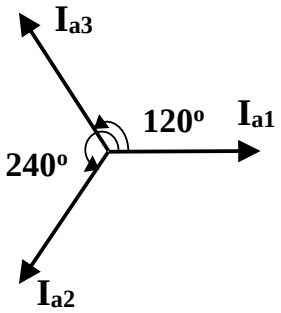

Fig 4.1 Proposed Harmonic pilots injection

4.2.2 Goertzel algorithm and DG failure detection

The Goertzel algorithm is used to monitor the Vpcc and line current of the 9th harmonic component to compute the DFT spectra. The computation of Goertzel algorithm for Nth – value of frequency is more efficient than direct computation of DFT [98] and it provides the magnitude and phase of the line currents and V_{pcc} at 9th harmonic frequency with nominal computation easily implementable on low-cost microcontrollers.

4.2.2.1 Detection of Grid failure

In the Microgrid, each DG unit plays the role of a 9th harmonic current source, injecting harmonics into the system, as discussed in the previous section. To create an islanded μG scenario, the grid circuit breaker (CB) is intentionally opened, disconnecting the Microgrid from the main utility grid. This isolation leads to the formation of an islanded μG. When the grid is disconnected, the harmonics generated by the DGs are compelled to flow through the loads connected at each PCC of the DGs within the islanded μG. This occurs because there is no longer a direct path for the harmonics to flow back to the main utility grid. Due to the different impedance characteristics in the islanded configuration compared to the grid-tied condition, the equivalent impedance offered by the μG increases. This change in impedance has a significant impact on the 9th harmonic content at the PCC of each DG. The increase in impedance causes the 9th harmonic component to become more pronounced at the PCC of each DG.

To identify and measure the amplification of the 9th harmonic component, the Goertzel algorithm is utilized to calculate the magnitude of the harmonic signal. This algorithm is integrated into the control system of each inverter present in the μG. By monitoring the magnitude of the 9th harmonic using the Goertzel algorithm, any

significant deviation from the normal operating conditions can be easily detected, allowing for appropriate corrective measures to be taken.

4.2.2.2 Detection of islanding of a particular DG in the µG

Let's denote the current phasors at the 9th harmonic of DG_1, DG_2, and DG_3 injected into the grid as I_{a1}, I_{a2}, and I_{a3}, respectively. Similarly, we'll use I_{ao1}, I_{ao2}, and I_{ao3} to represent the line currents at the 9th harmonic in the sections of the µG, and $I_{a\text{-}grid}$ to indicate the current flowing into the grid. We can approximate the relationship between these phasors as follows:

$$I_{ao3} = I_{a3} \tag{4.1}$$

$$I_{ao2} = I_{ao3} + I_{a2} \tag{4.2}$$

$$I_{ao1} = I_{ao2} + I_{a1} \tag{4.3}$$

$$I_{ao1} = I_{a-grid} \tag{4.4}$$

Likewise, we represent the voltages at the point of common coupling of DG_1, DG_2, and DG_3 as V_{pcc1}, V_{pcc2}, and V_{pcc3}, respectively. It's important to note that V_{pcc1} is zero when I_{ao1} is zero. Now, let's examine the relationship between the currents injected by the distributed generators (DGs) and the voltages at the PCC:

$$V_{pcc2} = I_{ao2} * (R_1 + R_2) \tag{4.5}$$

$$V_{pcc3} = \left(I_{ao2} * (R_1 + R_2)\right) + (I_{ao3} * R_2) \tag{4.6}$$

Fig 4.2 illustrates the voltage phasors, while Fig 4.3 depicts the current phasors during normal operation. In the event of a DG being isolated from the µG, the DGs located before the disconnected DG can detect the islanding by analysing the 9th harmonic current. Since the grid presents zero impedance to the 9th harmonic currents, the trailing DGs can identify the islanding by monitoring the 9th harmonic voltage at the point of common coupling (V_{pcc}).

Let's consider a scenario where DG_3 is disconnected from the grid. Prior to the disconnection of DG_3, the net 9th harmonic current injected into the grid (I_{ao1}) is zero. However, after DG_3 is disconnected, the net current being injected into the grid redistributes, now having a magnitude of $|I_{h9}|$ at 300˚. This new current magnitude and phase angle are exactly the negative of the harmonic previously injected by the disconnected DG_3. As a result, a phase shift and magnitude alteration become apparent

at V_{pcc}. We can observe the post-disconnection current phasors in Figure 4.4 and the voltage phasors in Figure 4.5.

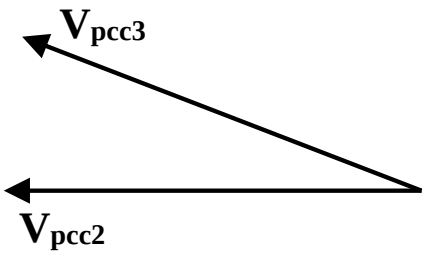

Fig 4.2 Voltage phasor under normal operation

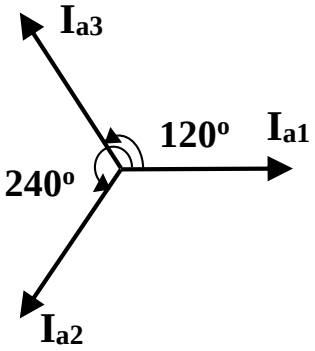

Fig 4.3 Current phasor under normal operation

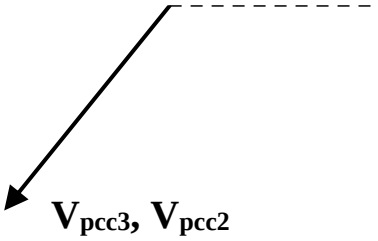

Fig 4.4 Voltage phasor when DG_3 is disconnected

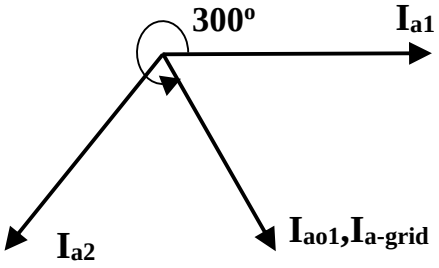

Fig 4.5 Current phasor when DG_3 is disconnected

4.3 FUZZY LOGIC BASED INFERENCING SYSTEM

The fuzzy inference system (FIS) is designed to autonomously process data obtained from voltage and current phasors at each node. In this study, a Type-1 Mamdani FIS is utilized due to its robustness in effectively communicating information about grid islanding and DG outages among interconnected DGs. This FIS demonstrates adaptivity and non-linearity, making it suitable for handling sudden changes in voltage or current sensing data [99].

Since the effectiveness of the fuzzy decision-making model is significantly influenced by the membership function's shape, a careful selection has been done to configure them as broader/thicker and thinner/narrower. The magnitudes and phases of the current and V_{pcc} at 9^{th} harmonic frequency have been computed using the Goertzel algorithm which is given as input to the Fuzzy inference system (FIS). Simple and intuitively clear triangular membership function is considered for inputs: angle_I_{aon} and angle_V_{pccn} in radian, where n is the n^{th} node and the output represents the islanding status of DGs and that of the μG from grid.

The fuzzy inference system is designed for three cases of operation of μG as shown in Table 4.2, Table 4.3 and Table 4.4 when observed from DG_1, DG_2 and DG_3 locations respectively. The Table 4.2 individually deals with observing the status of other DGs and normal operation of grid when observed from DG_1 location. Similarly, the Table 4.3 and Table 4.4 follows the suit respectively for DG_2 and DG_3 locations. The fuzzification membership function in accordance with Table 4.2, 4.3 and 4.4 is depicted in Fig 4.6, Fig 4.7 and Fig 4.8 respectively. The outage of multiple DGs is fuzzified in the overlapping area of output membership function as shown in Fig 4.6, Fig 4.7 and Fig 4.8 for respective DG locations. The main aim to make aware individually each DG autonomously about islanding condition of the grid and outages of interconnected DGs aids to better control the μG in both islanded and grid connected conditions. Fuzzy inferencing system assist the embedded control at each DGs based on locations of DG in leading or trailing position with respect to point of observation, i.e., DG_3 will know when DG_1 and/or DG_2 is disconnected to better amend the control of inverter. The advantage of the application of fuzzy logic inferencing system is fast detection of islanding condition and outages of other DGs, one or multiple at a time, i.e., detection of DG_1 and DG_2 together with reference to the considered μG. The fuzzy output at DG_1, DG_2 and

DG_3 is obtained after defuzzification as operating on output membership function at each DG is shown in Table 4.5, Table 4.6, and Table 4.7 respectively.

TABLE 4.2 CASES OF OPERATION OF DG_1

Cases	angle_I_{ao1}	Inference
Case 1	[-0.1 1.9]	Normal operation
Case 2	[-1.6 0]	DG_2 disconnected
Case 3	[-4.1 -0.6]	DG_3 disconnected

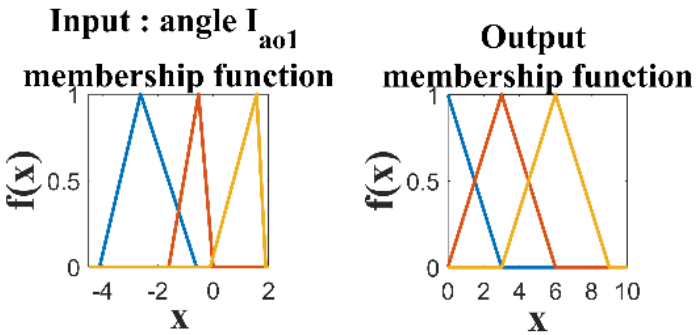

Fig 4.6 Input and output membership functions of DG_1

TABLE 4.3 CASES OF OPERATION OF DG_2

Cases	angle_ I_{ao2}	magn_V_{pcc2}	Inference
Case 1	[0 1.8]	[0 0.5]	Normal operation
Case 2	[0 1.8]	[0.97 1.5]	DG_1 disconnected
Case 3	[1.5 3]	[0.45 1.5]	DG_3 disconnected

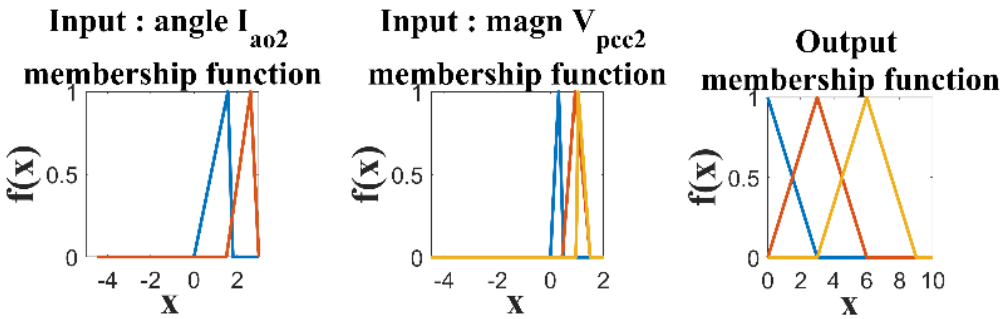

Fig 4.7 Input and output membership functions of DG_2

TABLE 4.4 CASES OF OPERATION OF DG_3

Cases	angle_V_{pcc3}	Inference
Case 1	[1.35 3.5]	Normal operation
Case 2	[0 1.4]	DG_1 disconnected
Case 3	[0 0.8]	DG_2 disconnected

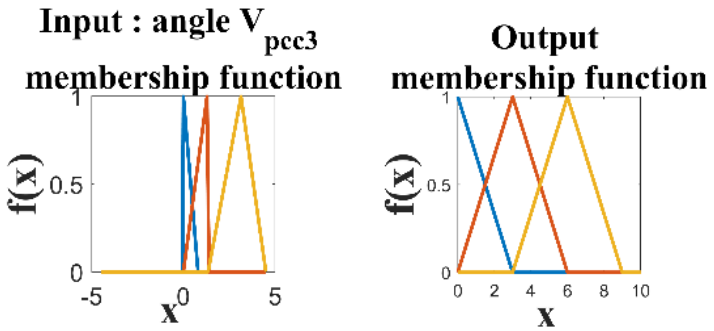

Fig 4.8 Input and output membership functions of DG_3

TABLE 4.5 OUTPUT MEMBERSHIP FUNCTION OF DG_1

Crisp number range	Condition of grid
[0 0 3]	Normal operation
[0 3 6]	DG2 is disconnected
[3 6 9]	DG3 is disconnected

TABLE 4.6 OUTPUT MEMBERSHIP FUNCTION OF DG_2

Crisp number range	Condition of grid
[0 0 3]	Normal operation
[0 3 6]	DG1 is disconnected
[3 6 9]	DG3 is disconnected

TABLE 4.7 OUTPUT MEMBERSHIP FUNCTION OF DG_3

Crisp number range	Condition of grid
[0 0 3]	Normal operation
[0 3 6]	DG1 is disconnected
[3 6 9]	DG2 is disconnected

Since the current at 9^{th} harmonic frequency adds up only in the forward direction since the grid offers no impedance to 9^{th} harmonic pilots, the DG_1 is the most leading, and DG_3 is the most trailing DG for the considered μG. Based on the proposed scheme of islanding detection, the DGs ahead of a disconnected DG would detect the islanding based on the 9^{th} harmonic V_{pcc} and trailing DGs would detect the disconnection by monitoring the 9^{th} harmonic current. When DG_1 is disconnected, the trailing DGs, i.e., DG_2 and DG_3 would observe the phase angle of V_{pcc2} and V_{pcc3} respectively. On the other hand, if DG_2 is disconnected, the trailing DG, i.e., DG_3 would observe the phase angle of V_{pcc3}, while for the leading DG, i.e., DG_1 will observe the phase angle of I_{ao1}. Similarly, DG_3 being the most trailing DG, the two leading DGs, i.e., DG_2 and DG_1 should observe the phase angle of I_{ao2} and I_{ao1} respectively. Accordingly, if-then cases formulated for all DG locations based on phase angle of both V_{pccn} and I_{aon} at respective point of common coupling for observation of normal operation and outage of all DGs in the μG.

The membership function for phase angle of I_{ao1} as shown in Fig 4.6 becomes unilateral in respect of outages of DG_2 and/or DG_3 as both the DGs lie on the trailing end of DG_1. However, both the input functions, namely, phase angle of I_{ao2} and magnitude of V_{pcc2} as shown in Fig 4.7, have been considered to develop the fuzzy inferencing system for DG_2 (DGs having both leading and trailing location of other DGs). The membership functions magn_V_{pcc2} and angle_ I_{ao2} are unilateral because magnitude in respect of former is always positive and later is detecting the outage of DG trailing to it. The membership function angle_V_{pcc3} as shown in Fig 4.8 is also unilateral being the most trailing DG detecting the outage of DGs ahead to it. The weight distribution of the membership function thus formed is chosen in a manner that the weights of I_{aon} and V_{pccn} at respective PCC accounting for the outage of multiple DGs constructing the output to fall exactly in the overlapping period of the triangles representing the outage corresponding to individual DGs distinguishing it from the normal condition of operation [100].

4.4 SIMULATION RESULTS

The theoretical analysis of the proposed islanding detection methodology is duly supported by simulation study under MATLAB/SIMULINK environment on the developed μG. The considered microgrid system has three DG sources with 3kW capacity, and 4kW load connected at each common coupling point. The line resistances

Z_1 and Z_2 are 0.48Ω and 0.73Ω representing 1.7km and 2.5km feeder line respectively. The line is assumed to be resistive owing to the R/X ratio greater than 7. The grid is modelled for 415V, 50Hz. Each DG is connected and/or disconnected with the grid through circuit breakers. Goertzel algorithm is modelled for a sampling frequency of 20kHz at a sampling rate of 2000 per cycle to detect 9^{th} harmonic components of 450Hz.

To amicably test the fuzzy inferencing system, the DG_3 is taken off from the grid intentionally. Both DG_1 and DG_2 are demonstrated to detect this condition through the current harmonic phasor as they are leading ahead in location to the disconnected DG_3. Under normal condition of operation, the 9^{th} harmonic current phasors depicted in Fig 10 duly shown as DG_1 (red), DG_2 (yellow), DG_3 (blue) and I_{ao1} (magenta)(the harmonic current flowing into the grid) to be zero. The 9^{th} harmonic voltage phasor under normal condition of operation is shown in Fig 11, which depicts the V_{pcc3} (red) and V_{pcc2} (yellow), complying with the theoretical calculations that V_{pcc1} is zero, due net zero 9^{th} harmonic component. The 9^{th} harmonic current phasors when DG_3 is disconnected is shown in Fig 12, where I_{ao1} (magenta) is shown non – zero having finite magnitude, points in the direction opposite to the phasor that was injected by DG_3 before disconnection. The voltage phasors post disconnection of DG_3 is shown in Fig 13. The simulated result on the polar plots confirms the proposed algorithm for assessment of outage of DG_3 respectively.

Further to evaluate the efficacy of the proposed fuzzy inferencing system working in tandem with outputs of Goertzel algorithm based assessment, the triangular membership functions as shown in Fig 4.6, Fig 4.7, and Fig 4.8, for DG_1, DG_2 and DG_3 respectively are formulated using Fuzzy logic toolbox in MATLAB/Simulink environment to fuzzify and defuzzify for drawing the phasor inference based on V_{pcc1}, V_{pcc2}, I_{ao1} and I_{ao2}. Two instances: case1: normal functioning of the μG and case2: when DG_3 is islanded from the μG have been processed. The output of fuzzy inference system draws out for DG_1, DG_2 and DG_3 locations is 0.9667, 1.0000 and 1.4635 respectively which when referred with, TABLE 4.5, TABLE 4.6 and TABLE 4.7 respectively, confirm normal operating condition. While the proposed algorithm draws out crisp values in the latter case as 5.6998 and 6.0000 at DG_1 and DG_2 locations respectively, indicating the disconnection of DG_3 when referred with TABLE 4.5 and TABLE 4.6. To further probe the efficacy of the proposed inferencing system, a case when both DG_3 and DG_2 are disconnected is considered, the fuzziness in FIS at DG_1 detects a value of 4.2075 which

lies in the intersection zone of detection of islanding condition of DG_2 and DG_3 as referred in TABLE 4.5 and Fig 4.6. Thus clear cut detection of the outage of DG_3, bring merit to the proposed inferencing system to add the control of the other DGs connected to the µG for mostly the power requirements of the connected loads based for reliable and efficient operation of the µG irrespective of grid disconnections and outages of DGs by better planning of the control by increasing the deloading efficiency by making better use of the remaining connected DG sources by operating close to MPPT and imparting adequate inertial response.

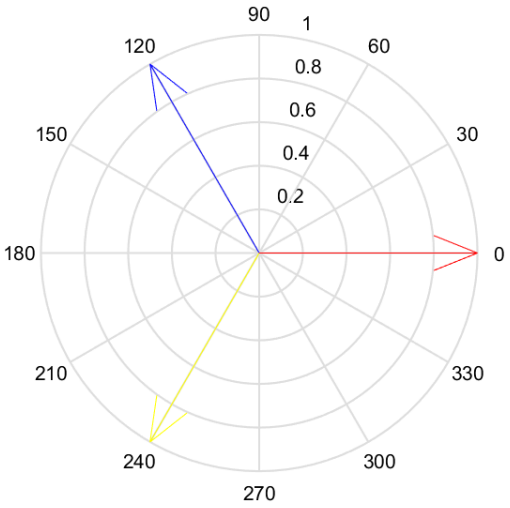

Fig 4.9 9th harmonic current phasor under normal operation

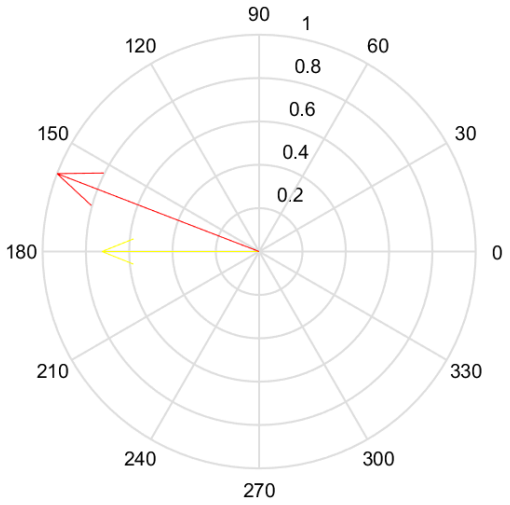

Fig 4.10 9th harmonic Voltage phasor under normal operation

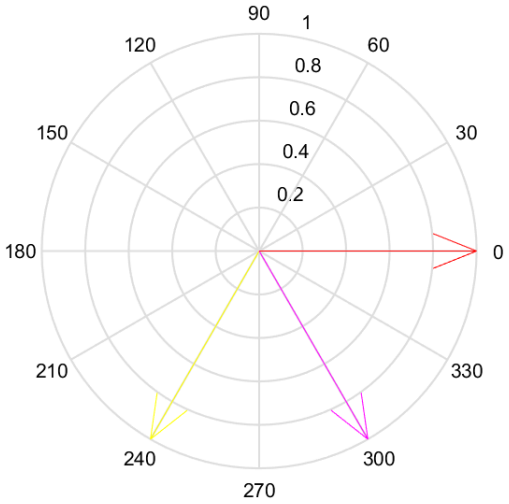

Fig 4.11 9th harmonic Current phasor when DG3 is disconnected

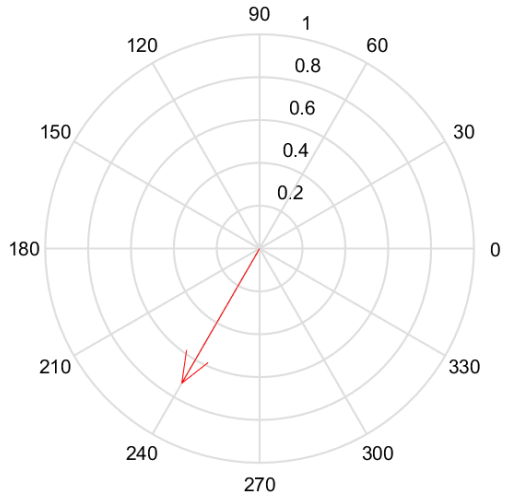

Fig 4.12 9th harmonic Voltage phasor when DG3 is disconnected

4.4 RESULTS AND DISCUSSION

The proposed Goertzel algorithm-based grid islanding cum DG outage detection technique incorporating fuzzy inferencing system has been verified using MATLAB/Simulink based results. The results successfully demonstrate fast, accurate and reliable detection of grid islanding and/or outage of the DGs in the µG aiding to control of inverters for seamless transit between grid – tied mode to islanded mode with efficient planning for matching generated power with the load for working efficiently in islanded operation of µG and prevention of reverse power flow to preserve the efficacy of existing protection scheme. The proposed methodology simple, effective, advantageous and aids efficient energy generation through robust and autonomous control at each inverter location without any complex and costly communication infrastructure.

One drawback of fuzzy inference systems (FIS) is their vulnerability to noise in the input data. Noise refers to random variations or disturbances that can affect the accuracy and reliability of the data being processed by the FIS. Fuzzy inference systems rely on membership functions and fuzzy rules to make decisions based on the input data. However, when the input data contains noise, it can lead to imprecise or incorrect decisions by the FIS. Noise can introduce unpredictable variations in the input values, which may cause the FIS to assign incorrect membership degrees to different fuzzy sets or misinterpret the data.

The presence of noise in the input data can result in fuzzy sets overlapping or blending, making it challenging to accurately determine the membership degrees. This can lead to inaccurate fuzzy rule activation and subsequent incorrect decision-making by the FIS. To mitigate the impact of noise, it is crucial to pre-process the input data by applying noise reduction techniques such as filtering or smoothing. These techniques aim to reduce or eliminate the noise present in the data before feeding it into the FIS. By minimizing the effects of noise, the FIS can make more reliable and accurate decisions. However, that would make the complete system more complex. Hence, to address this shortcoming, islanding detection algorithm employing wavelet packet decomposition has been proposed in the next chapter.

CHAPTER 5

ISLANDING DETECTION USING WAVELET PACKET TRANSFORM

5.1 PROPOSED METHODOLOGY

This chapter proposes an islanding detection method utilising DG tagging strategy that is reliable, effective, and fast when multiple DG's are present in a μG and detection is responsible not only for grid islanding but also DG's outages. The proposed method involves the injection of 9^{th} harmonic pilots, which can quickly identify grid islanding, along with the outage of specific DGs. The wavelet packet method (WPT) is used at each node in autonomous mode to observe the 9^{th} harmonic component of the voltage at Point of Common Coupling (PCC) in conjunction with the current in the line around each node, including the node which is transacting power with the grid interface. The injected balanced 9^{th} harmonic currents are set to a fixed value and sum up vectorially at the grid interfaced node to a zero value under normal conditions of operation. Being equi-displaced in phase with respect to one another, it is likely to introduce minimal harmonic impact on account of their escape to mainly the grid by each DG. By observing the current and/or voltage signatures during grid – tied mode and various DG outage conditions, we can infer the condition of the grid. This method overcomes the shortcoming of the previously proposed method, i.e., it overcomes the inaccuracy that can be caused due to noise amplification. Also, it addresses the heavy cumbersome process involved in computation when using fuzzy inferencing system when multiple DGs are connected in the grid.

5.2 SYSTEM UNDER STUDY

The single line diagram of the μG used for analysis and design in this study is shown in Fig1. The μG consists of 3 photovoltaic-fed inverter DER's, each with a maximum power rating of 3kW, connected to the 415V distribution grid, and injecting power at unity power factor through their respective PCCs in GSM. At each PCC node, there is a local load of 4kW. The utility distribution network is modelled with an AC

source of 415V, 50Hz, and lumped line impedance Z_{line1} and Z_{line2} to evaluate the proposed islanding detection algorithm efficiency. The line impedance between the two sources is considered resistive, as it operates at low voltage levels, and the voltage at PCC(V_{pcc}) of each DG is in approximately the same phase as the others due to minimum line reactance.

5.2.1 Harmonic Component Injection

Since the considered system is 3-phase 4-wired, the 3rd harmonic and its odd multiple current flow through the neutral wire but balance out in the line. Therefore, to enable islanding detection, harmonic pilots of the order 3n(where n = 1,3,5,7…) can be injected into the line. In this paper, 9th harmonic current and/or voltage pilots are used as a unique signature for detecting islanding events since these are not commonly present in the power system under normal operating conditions but also because their frequency being high enough to be easily distinguished from the fundamental frequency, but low enough to avoid significant signal attenuation in the power system. The phase angle between the 9th harmonic current injected by the three DGs is calculated to be 120˚(360˚/n), where n is equal to 3, as the system is 3-phase. For this discussion, the focus will be on the single-phase current and voltage phasers, with the understanding that the same logic applies to the other two phases. The first DG, i.e., DG_1 injects current at the 9th harmonic at 0˚, while DG_2 injects current at 240˚ and DG_3 at 120˚ respectively. The sum of the three harmonic current phasors at the 9th harmonic adds up to zero, resulting in a net harmonic current of zero injected into the grid.

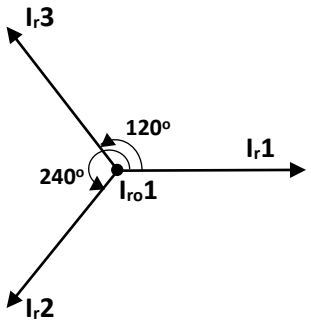

Fig 5.1 Proposed 9th Harmonic pilots' injection

5.2.2 DG failure detection

The current phasors at the 9th harmonic injected by DG_1, DG_2 and DG_3 into one phase, say r-phase of the grid can be represented as I_{r1}, I_{r2} and I_{r3}. Similarly, I_{ro1}, I_{ro2}, and I_{ro3}, are the line currents of one phase at the 9th harmonic in the sections of the μG,

while I_{r_grid} denotes the current flowing into the grid. The relation between the above phasors can be approximated as follows:

$$I_{ro3} = I_{r3} \tag{5.1}$$

$$I_{ro2} = I_{ro3} + I_{r2} \tag{5.2}$$

$$I_{ro1} = I_{ro2} + I_{r1} \tag{5.3}$$

$$I_{ro1} = I_{r-grid} \tag{5.4}$$

Similarly, the voltages at the PCC(V_{pocc}) of DG_1, DG_2 and DG_3 are depicted as V_{pocc1}, V_{pocc2}, and V_{pocc3} respectively. Under normal condition of operation, V_{pocc1} is zero, because the net harmonic 9th harmonic current, I_{ro1} flowing into the grid is zero. The relation between the PCC voltages and currents injected by each DG are as follows:

$$V_{pocc2} = I_{ro2} * (Z_{line1} + Z_{line2}) \tag{5.5}$$

$$V_{pocc3} = \left(I_{ro2} * (Z_{line1} + Z_{line2})\right) + (I_{ro3} * Z_{line2}) \tag{5.6}$$

In the event of a DG being isolated from the μG, the DGs upstream of the disconnected DG would detect the islanding by analysing the 9th harmonic current. Since the grid offers zero impedance to the 9th harmonic currents, the current only adds up in the forward direction. The DGs downstream of the isolated DG would detect the islanding by monitoring the 9th harmonic V_{pocc}, as the voltage phasors would not add up to zero due to absence of the current phasor that was previously being injected by the isolated DG. Consider a case where DG_2 disconnects from the μG. The DGs upstream of the disconnected DG, i.e., DG_1 would know about it by observing the change in current phasor, while the DGs downstream, i.e., DG_3 would know of its disconnection by analysing the voltage phasor at its PCC. This method of islanding detection creates an opportunity for implementation of communication system failure proof islanding detection infrastructure, which is more reliable, cost – effective and free from communication delays, thereby reducing the time taken to implement the corrective measures.

5.2.3 Wavelet packet decomposition implementation

Wavelet packet decomposition is a useful signal processing tool that helps in islanding detection owing to its ability to effectively detect changes induced in the high frequency components of voltage and current signals post occurrence of islanding event. Compared to Fourier-based transforms such as STFT, FFT, and DFT, the wavelet transform offers several advantages. This is primarily because of the window size is

fixed in Fourier based transforms, while it varies in wavelet transform. Therefore, time frequency resolutions are not compromised in wavelet transform. Additionally, the computational ability of wavelet packet transforms to ably determine time and frequency information for low and high frequencies using long and short windows respectively can be used to merit in accurate islanding detection, where grid possesses various multiple current and voltage harmonic pilots.

The current and voltages at PCC of each DGs are analysed by decomposing into its wavelet packets at various scales and frequencies using the Tree Decomposition algorithm. Sampling frequency($f_{sampling}$) of 10KHz has been used to sample the currents and voltages of the proposed system to demonstrate the efficacy of the proposed algorithm. According to Nyquist sampling theorem, the topmost frequency signal of the binary tree is $f_{sampling}/2$, i.e., 5KHz. This signal is split into two sub bands: the approximation coefficients(low pass filtered signal), i.e., signal in the range 0-2.5 KHz and the detail coefficients(high pass filtered signal) i.e., signal in the range 2.5-5 KHz. This tree decomposition method is further recursively applied to the splitting process to update the approximation coefficients until the desired number of decomposition levels is reached, where the tree is pruned to remove the unnecessary sub bands, such that 50 Hz in 450 Hz signals are distinctively separated as shown in Fig 5.2. The simplicity in the tree structure as shown in Fig 5.2 allows for accurate and detailed analysis compared to the Fourier-based methods.

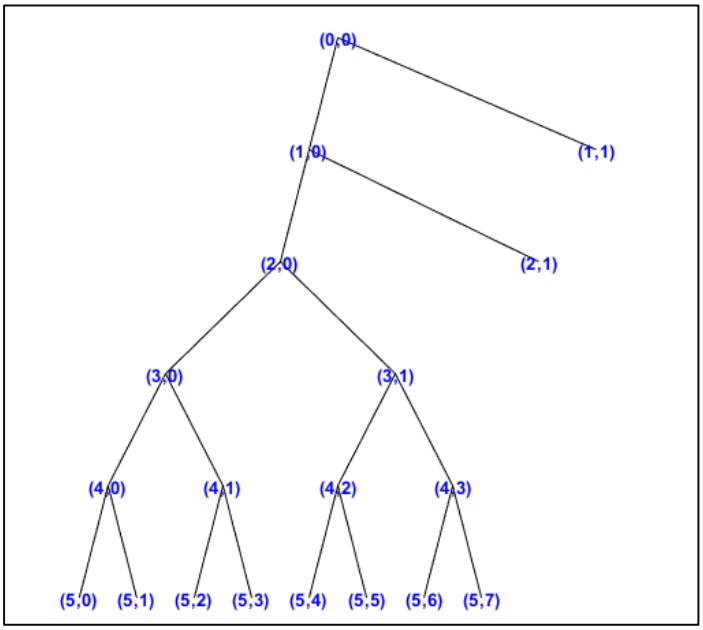

Fig5.2 Pruned Binary tree structure depicting the signal decomposition

Thus, 5-level binary tree-decomposition has been implemented which distinctively identifies the current and voltage signatures of 50Hz and 450 Hz pilots at (5,0) or 31 and (5,2) or 33 sub-bands respectively. By observing the 450Hz current and/or voltage pilots' signature at the respective PCC, information regarding islanding of other DGs in a network can be known, which therefore will help it to manage its power generation capability to meet the load demand. Islanding of different DGs in the system produce unique 450Hz current and/or voltage signatures, which are analysed based on the location of the DG with respect to the disconnected DG.

Consider a case when DG_2 is disconnected from the grid. Disconnection of DG_2 is known to DG_1 by analysing the 450Hz current signature of I_{ro1} at its PCC, since it being a upstream DG. Similarly, DG_3 would know of disconnection of DG_2 by analysing the 450Hz voltage signature of V_{pocc3} at its PCC, since it being a downstream DG in the system. If both DG_2 and DG_3 are disconnected, then the unique current signature of I_{ro1} at the PCC of DG_1 can be used to infer the islanding.

5.3 RESULTS AND DISCUSSION

To support the theoretical analysis of the proposed islanding detection technique, a simulation study was implemented in MATLAB/SIMULINK environment on the proposed microgrid system. The microgrid consists of three DER's with the capacity of 4.2 kW supplying a 5.67 kW load connected to each PCC. The line resistances, represented by Z_{line1} and Z_{line2} are 0.467Ω and 0.783Ω, respectively which corresponds to feeder line distances off 1.7 km and 2.5 km. The line is assumed to be resistive with a resistance to reactance ratio greater than 7. The grid is modelled at 415V and 50Hz. The connection and disconnection of each DG to the grid is implemented through circuit breakers. The wavelet packet decomposition is implemented on signals sampled at 10KHz . A 5-level binary tree decomposition approach is implemented to separate the various sub-bands in the signal, in order to distinctly capture the 450Hz signal component being analysed. I_{ro1} current waveform when system is operating under normal operation, when DER_2 is disconnected, when DER_3 is disconnected and when both DER's are disconnected are as shown in Fig 4, Fig 5, Fig 6, and Fig 7 respectively. Fig 5, Fig 6, and Fig 7, depict the disconnection of DER's from the system evidently. Thus, current signatures method of islanding detection is implemented.

The Symlet 8(Sym8) wavelet is used in islanding detection because it has a good balance between time and frequency localization, making it suitable for detecting

small changes in the signal overtime during islanding detection procedure. Additionally, the Sym8 wavelet has a higher number of vanishing moments compared to other commonly used wavelets, which allows for better suppression of noise and better signal reconstruction after wavelet packet decomposition, compensating the shortcoming of the Fuzzy inferencing system methodology [26].

The I_{ro1} 9^{th} harmonic sub-band under normal operation is shown in Fig 8. Fig 8 has a magnitude of zero, because, under normal condition of operation, all the 9^{th} harmonic components add up to zero, indicating absence of islanding. The 9^{th} harmonic sub-band of I_{ro1} when DG_2 is islanded is shown in Fig 9. The 9^{th} harmonic sub-band current signature of I_{ro1} when DG_3 is islanded is shown in Fig 10. The 9^{th} harmonic sub-band current signature in the above two cases is different, owing to the harmonic pilots' injection method proposed in section 3. The phase displacement introduced during current pilot injection leads to the acquisition of distinct and individual signatures within the current waveforms. The I_{ro1} 9^{th} harmonic sub-band current signature when both DER_2 and DER_3 are islanded shown in Fig 11, is different to that shown in Fig 8, Fig 9 and Fig 10. The same analysis can be applied for the detection of islanding of upstream DER's by detecting the V_{pocc} at the respective PCC of the DGs lying downstream of the disconnected DG. Since this method does not require any communication infrastructure, the ratio of accuracy of detection to the cost of implementation is very high. The results obtained from the proposed method can be further fed to ANN algorithm, which can help identify the non-linearities in data considered for islanding detection, making it even better adaptable islanding detection solution.

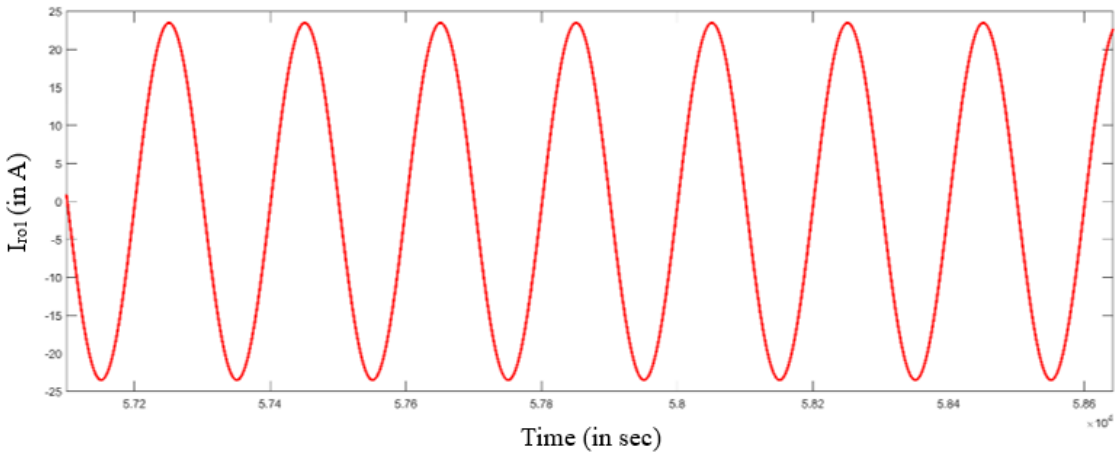

Fig 5.3 I_{ro1} waveform under normal condition of operation

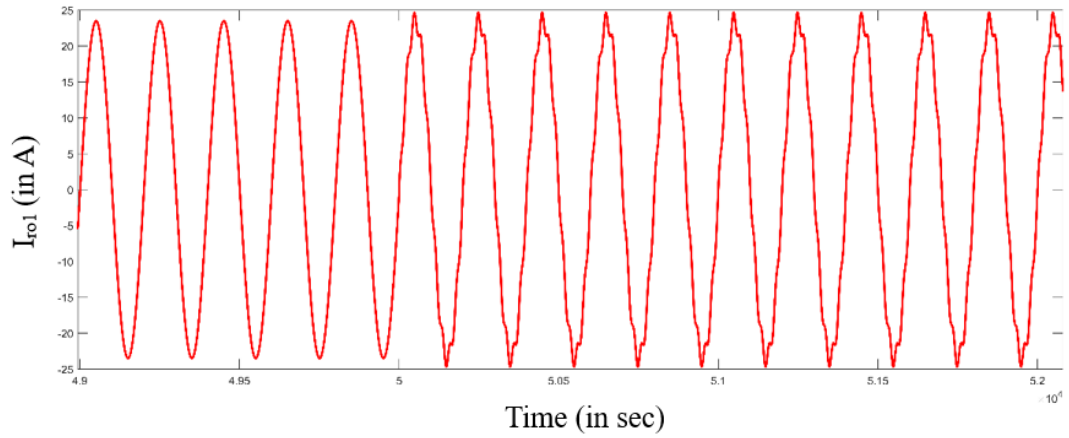

Fig 5.4 I_{ro1} waveform when DG_2 is disconnected

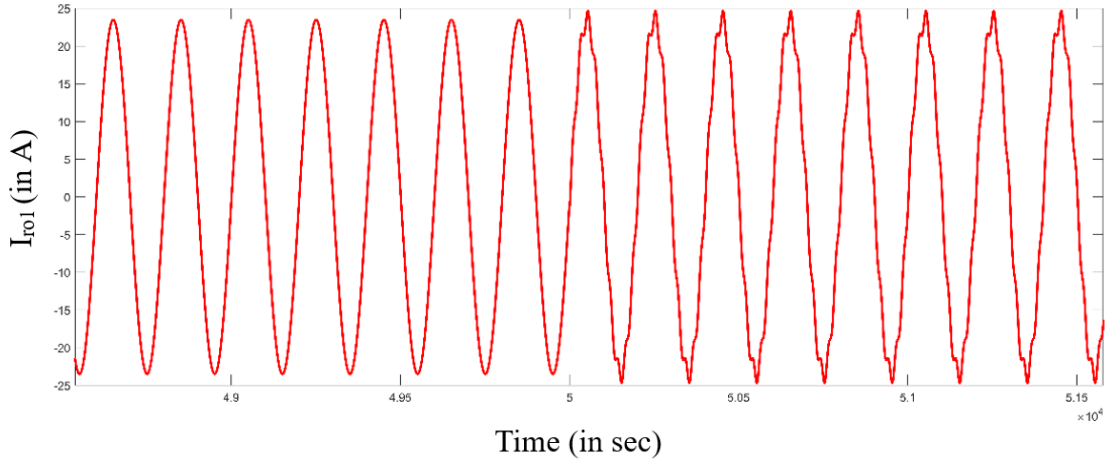

Fig 5.5 I_{ro1} waveform when DG_3 is disconnected

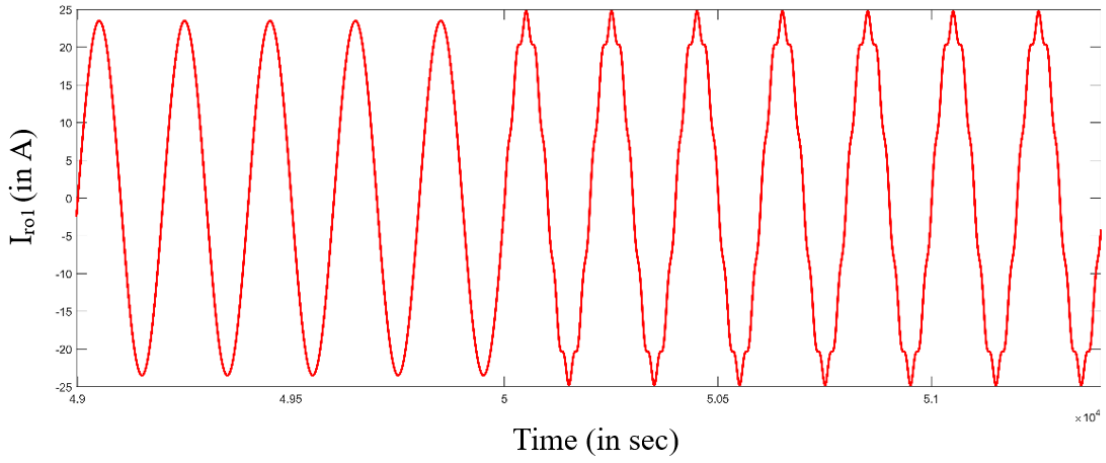

Fig 5.6 I_{ro1} waveform when both DG_2 and DG_3 are disconnected

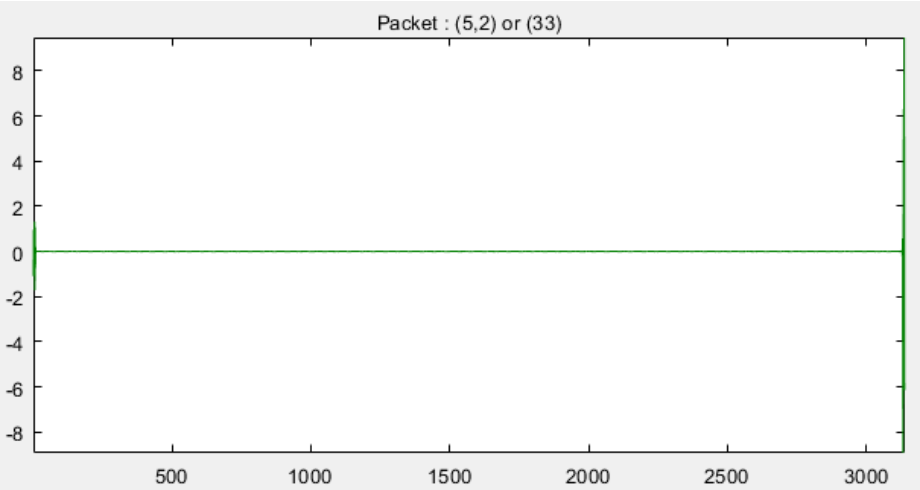

Fig 5.7 9th harmonic sub-band of I_{ro1} waveform under normal condition of operation

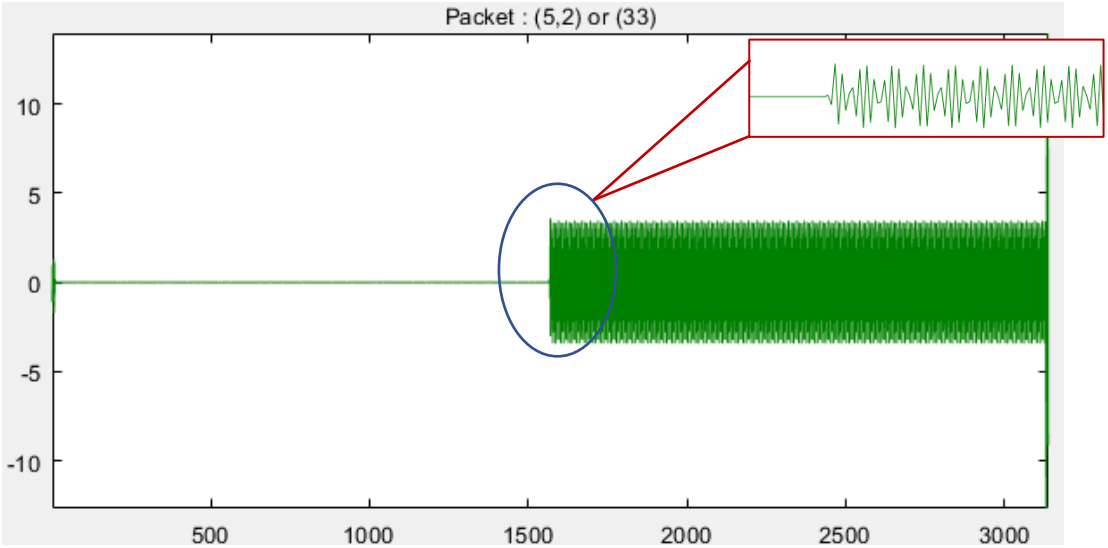

Fig 5.8 9th harmonic sub-band of I_{ro1} waveform when DG_2 is disconnected

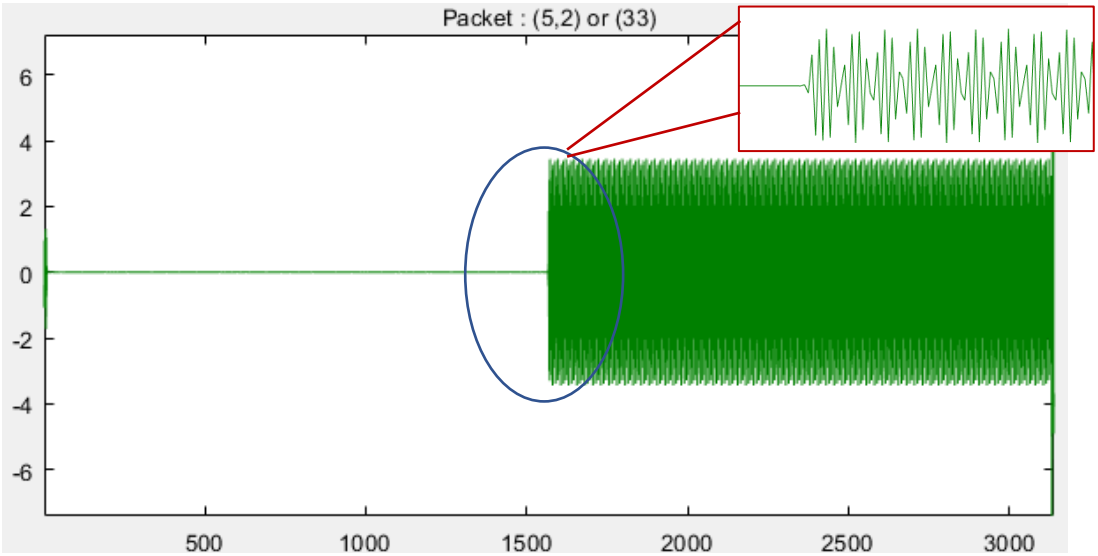

Fig 5.9 9th harmonic sub-band of I_{ro1} waveform when DG_3 is disconnected

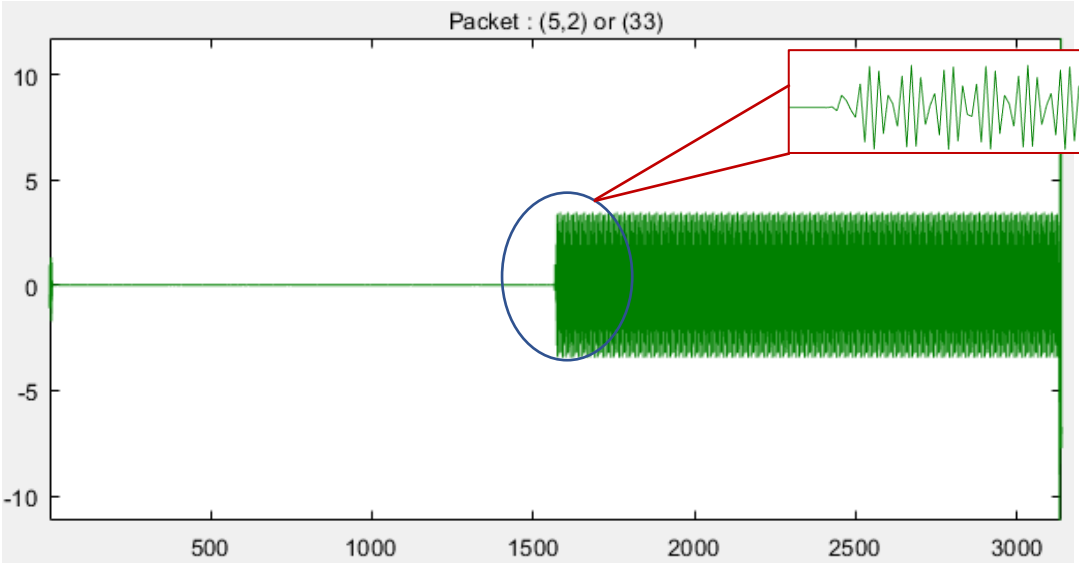

Fig 5.10 9^{th} harmonic sub-band of I_{ro1} waveform when both DG_2 and DG_3 are disconnected

CHAPTER 6

CONCLUSION AND FUTURE SCOPE OF WORK

To address the protection needs arising due to the increased penetration of renewable energy sources into the grid, robust, accurate, fast and cost-effective islanding detection solutions become vital. These ensure proper functioning of the grid and improve the reliability of the power supply. With a reliable and resilient grid, the surplus energy generated from distributed energy resources can be fed to the grid. The various islanding detection methods previously suggested in literature have been carefully studied and explained in Chapter 2. The shortcomings of various methods have been highlighted, and an effort has been put to come up with an even better solution, addressing the technology gap and to always stand by the islanding detection standards as mentioned in Chapter 1.

This thesis project investigated two islanding detection methods: The first one incorporating Goertzel algorithm in collaboration with fuzzy inference system (FIS) and the other one discussing the application of wavelet packet transform (WPT) in islanding detection where multiple DGs are connected. The objective was to address the limitations of the FIS method with the WPT method, ultimately providing a robust and communication-independent solution for islanding detection.

The FIS method, however effective in modelling complex relationships and uncertainties, encounters challenges in accurately analysing transient events and disturbances in power system signals. Also, when there are multiple DGs connected in the grid, this method requires large computation, thereby making the implementation process complex. By adapting the WPT method, which decomposes signals into different frequency sub-bands, the shortcomings of the FIS method were successfully addressed, because even in the presence of multiple DGs, and multiple other unwanted harmonics, due to this division of frequencies into sub-bands makes this islanding detection method less complex. The WPT method captures unique signatures of current and voltages associated with islanding events, improving the accuracy and reliability of

the detection processes. The simulation results obtained in this thesis project supported the effectiveness of the combined approach.

Moreover, both the FIS and WPT methods were found to be independent of a communication system. This is a crucial advantage as it eliminates the need for additional infrastructure and reduces dependency on external communication networks. The independence of these methods from communication systems enhances their applicability and reliability in real-world power systems. The findings of this thesis project contribute to the field of islanding detection by providing a comprehensive and communication-independent solution. The research outcomes have practical implications for power system protection, as the proposed methods can be implemented in various power system environments without the requirement of complex communication infrastructure.

6.1 FUTURE SCOPE OF THIS WORK

The thesis project on the two IDMs, fuzzy inference system (FIS) and wavelet packet transform (WPT), opens up several future avenues for research and development. Despite addressing the shortcomings of the FIS method through the incorporation of the WPT method, there are still areas that can be explored to further improve the islanding detection techniques. The following are potential future scopes for this thesis project:

1. Enhancing the combined approach: Further optimization and refinement of the combined FIS and WPT method can be pursued to improve the accuracy and robustness of islanding detection. This could involve exploring different fuzzy logic rule sets and membership functions within the FIS, as well as investigating alternative wavelet bases and decomposition levels in the WPT. The goal would be to identify optimal configurations that maximize the detection performance.

2. Integration with advanced machine learning techniques: The combination of FIS and WPT with advanced machine learning algorithms, such as deep learning or reinforcement learning, could be explored. These techniques have shown promising results in various domains and could potentially enhance the islanding detection accuracy by leveraging the ability of neural networks to learn complex patterns and relationships from large datasets.

3. Real-time implementation and hardware optimization: The thesis project primarily focused on simulation-based evaluations. A future direction would involve

implementing the proposed islanding detection methods in real-time power system environments. This would require considering hardware constraints, such as limited computational resources and memory, and optimizing the algorithms for efficient execution on embedded systems.

5. Validation and comparison with other islanding detection techniques: It would be beneficial to compare the performance of the combined FIS and WPT method with other existing islanding detection techniques. This could involve benchmarking against rule-based approaches, machine learning-based methods, or state estimation techniques to evaluate the strengths and limitations of the proposed method in comparison to alternative approaches.

6. Integration with smart grid technologies: With the advancements in smart grid technologies, the integration of IDMs with intelligent control and communication systems presents a promising direction. Investigating how the WPT method can be integrated into a larger smart grid framework, incorporating advanced control algorithms and bidirectional communication, could enhance the overall resilience and reliability of the power system.

REFERENCES

1. J. A. P. Lopes, C. L. Moreira and A. G. Madureira, "Defining control strategies for MicroGrids islanded operation," in IEEE Transactions on Power Systems, vol. 21, no. 2, pp. 916-924, May 2006, doi: 10.1109/TPWRS.2006.873018.
2. J. Liang, T. C. Green, G. Weiss and Q. . -C. Zhong, "Hybrid control of multiple inverters in an island-mode distribution system," IEEE 34th Annual Conference on Power Electronics Specialist, 2003. PESC '03., Acapulco, Mexico, 2003, pp. 61-66 vol.1, doi: 10.1109/PESC.2003.1218274.
3. V. Verma and G. G. Talpur, "Decentralized Master-Slave operation of microgrid using current controlled distributed generation sources," 2012 IEEE International Conference on Power Electronics, Drives and Energy Systems (PEDES), 2012, pp. 1-6, doi: 10.1109/PEDES.2012.6484502.
4. IEEE Std. 100-2000 "Standard Dictionary of Electrical and Electronic Terms".
5. IEEE Standard for Interconnection and Interoperability of Distributed En[1]ergy Resources with Associated Electric Power Systems Interfaces, IEEE Standard 1547-2018 (Revision IEEE Standard 1547-2003), pp. 1–138, 2018.
6. "UL standard for inverters, converters, controllers and interconnection system equipment for use with distributed energy resources," UL 1741, Ed. 3, Sep. 2021.
7. R. Anne, F. Katha Basha, R. Palaniappan, K. L. Oliver and M. J. Thompson, "Reliable Generator Islanding Detection for Industrial Power Consumers With On-Site Generation," in *IEEE Transactions on Industry Applications*, vol. 52, no. 1, pp. 668-676, Jan.-Feb. 2016, doi: 10.1109/TIA.2015.2466560.
8. A. Pouryekta, V. K. Ramachandaramurthy, N. Mithulananthan and A. Arulampalam, "Islanding Detection and Enhancement of Microgrid Performance," in IEEE Systems Journal, vol. 12, no. 4, pp. 3131-3141, Dec. 2018, doi: 10.1109/JSYST.2017.2705738.
9. G. Bayrak, ‘‘A remote islanding detection and control strategy for photovoltaic-based distributed generation systems,’’ Energy Convers. Manage., vol. 96, pp. 228–241, May 2015, doi: 10.1016/j.enconman.2015.03.004.

10. G. Bayrak and E. Kabalci, ‘‘Implementation of a new remote islanding detection method for wind–solar hybrid power plants,’’ Renew. Sustain. Energy Rev., vol. 58, pp. 1–15, May 2016, doi: 10.1016/j.rser.2015.12.227.
11. K.-L. Chen, Y. Guo, J. Wang, and X. Yang, ‘‘Contactless islanding detection method using electric field sensors,’’ IEEE Trans. Instrum. Meas., vol. 70, pp. 1–13, 2021, doi: 10.1109/TIM.2020.3043096.
12. H. Samet, F. Hashemi, and T. Ghanbari, ‘‘Minimum non detection zone for islanding detection using an optimal artificial neural network algorithm based on PSO,’’ Renew. Sustain. Energy Rev., vol. 52, pp. 1–18, Dec. 2015, doi: 10.1016/j.rser.2015.07.080.
13. W. Xu, G. Zhang, C. Li, W. Wang, G. Wang and J. Kliber, "A Power Line Signaling Based Technique for Anti-islanding Protection of Distributed Generators: Part I: Scheme and Analysis," 2007 IEEE Power Engineering Society General Meeting, Tampa, FL, USA, 2007, pp. 1-1, doi: 10.1109/PES.2007.385448.
14. M. Ropp, D. Larson, S. Meendering, D. McMahon, J. Ginn, J. Stevens, W. Bower, S. Gonzalez, K. Fennell, and L. Brusseau, ‘‘Discussion of a power line carrier communications-based anti-islanding scheme using a commercial automatic meter reading system,’’ in Proc. IEEE 4th World Conf. Photovoltaic Energy Conf., May 2006, pp. 2351–2354.
15. J. Yang, J. Yuan, and S. Lin, ‘‘The study on island detection for distributed power combining power line zero-crossing communication technology,’’ in Proc. 7th IEEE Int. Conf. Electron. Inf. Emergency Commun. (ICEIEC), Jul. 2017, pp. 304–307, doi: 10.1109/ICEIEC.2017.8076568.
16. C. I. Chen and Y. C. Chen, ‘‘Intelligent identification of voltage variation events based on IEEE Std 1159-2009 for SCADA of distributed energy system,’’ IEEE Trans. Ind. Electron., vol. 62, no. 4, pp. 2604–2611, Apr. 2015, doi: 10.1109/TIE.2014.2348948.
17. E. Lazar, R. Etz, D. Petreus, T. Patarau, and I. Ciocan, ‘‘SCADA development for an islanded microgrid,’’ in Proc. IEEE 21st Int. Symp. Design Technol. Electron. Packag. (SIITME), Oct. 2015, pp. 147–150, doi: 10.1109/SIITME.2015.7342314.

18. D. Mlakic, H. R. Baghaee, and S. Nikolovski, ‘‘Gibbs phenomenonbased hybrid islanding detection strategy for VSC-based microgrids using frequency shift, THDU , and RMSU ,’’ IEEE Trans. Smart Grid, vol. 10, no. 5, pp. 5479–5491, Sep. 2019, doi: 10.1109/TSG.2018.2883595.
19. C. Li, C. Cao, Y. Cao, Y. Kuang, L. Zeng, and B. Fang, ‘‘A review of islanding detection methods for microgrid,’’ Renew. Sustain. Energy Rev., vol. 35, pp. 211–220, Jul. 2014, doi: 10.1016/j.rser.2014.04.026.
20. A. G. Abokhalil, A. B. Awan, and A. R. Al-Qawasmi, ‘‘Comparative study of passive and active islanding detection methods for PV gridconnected systems,’’ Sustainability, vol. 10, no. 6, p. 1798, 2018, doi: 10.3390/su10061798.
21. A. Etxegarai, P. Eguía, and I. Zamora, ‘‘Analysis of remote islanding detection methods for distributed resources,’’ Renew. Energy Power Qual. J., pp. 1142–1147, May 2011, doi: 10.24084/repqj09.580.
22. R. A. Walling, ‘‘Application of direct transfer trip for prevention of DG islanding,’’ in Proc. IEEE Power Energy Soc. Gen. Meeting, Jul. 2011, pp. 5–7, doi: 10.1109/PES.2011.6039727.
23. B. K. Panigrahi, A. Bhuyan, J. Shukla, P. K. Ray, and S. Pati, ‘‘A comprehensive review on intelligent islanding detection techniques for renewable energy integrated power system,’’ Int. J. Energy Res., vol. 45, no. 10, pp. 14085–14116, 2021, doi: 10.1002/er.6641.
24. M. Hojabri, U. Dersch, A. Papaemmanouil, and P. Bosshart, ‘‘A comprehensive survey on phasor measurement unit applications in distribution systems,’’ Energies, vol. 12, no. 23, p. 4552, 2019, doi: 10.3390/en12234552.
25. D. M. Laverty, R. J. Best, and D. J. Morrow, ‘‘Loss-of-mains protection system by application of phasor measurement unit technology with experimentally assessed threshold settings,’’ IET Gener. Transmiss. Distrib., vol. 9, no. 2, pp. 146–153, Jan. 2015, doi: 10.1049/iet-gtd.2014.0106.
26. M. M. Ostojić and M. B. Djurić, ‘‘The algorithm with synchronized voltage inputs for islanding detection of synchronous generators,’’ Int. J. Electr. Power Energy Syst., vol. 103, pp. 431–439, Dec. 2018, doi: 10.1016/j.ijepes.2018.06.023.
27. D. Kumar and P. S. Bhowmik, ‘‘Artificial neural network and phasor databased islanding detection in smart grid,’’ IET Gener., Transmiss. Distrib., vol. 12, no. 21, pp. 5843–5850, 2018, doi: 10.1049/iet-gtd.2018.6299.

28. X. Liu, D. M. Laverty, R. J. Best, K. Li, D. J. Morrow, and S. McLoone, ‘‘Principal component analysis of wide-area phasor measurements for islanding detection—A geometric view,’’ IEEE Trans. Power Del., vol. 30, no. 2, pp. 976–985, Apr. 2015, doi: 10.1109/TPWRD.2014.2348557.
29. S. Barczentewicz, T. Lerch, A. Bień, and K. Duda, ‘‘Laboratory evaluation of a phasor-based islanding detection method,’’ Energies, vol. 14, no. 7, p. 1953, Apr. 2021, doi: 10.3390/en14071953.
30. S. Murugesan and V. Murali, ‘‘Active unintentional islanding detection method for multiple-PMSG-based DGs,’’ IEEE Trans. Ind. Appl., vol. 56, no. 5, pp. 4700–4708, Sep. 2020, doi: 10.1109/TIA.2020.3001504.
31. J. J. Justo, F. Mwasilu, J. Lee, and J.-W. Jung, ‘‘AC-microgrids versus DC-microgrids with distributed energy resources: A review,’’ Renew. Sustain. Energy Rev., vol. 24, pp. 387–405, Aug. 2013, doi: 10.1016/j.rser.2013.03.067.
32. M. Hamzeh, S. Farhangi, and B. Farhangi, ‘‘A new control method in PV grid connected inverters for anti-islanding protection by impedance monitoring,’’ in Proc. 11th Workshop Control Modeling Power Electron., Aug. 2008, pp. 3–7, doi: 10.1109/COMPEL.2008.4634664.
33. P. Yazdkhasti and C. P. Diduch, ‘‘An islanding detection method based on measuring impedance at the point of common coupling,’’ in Proc. IEEE 28th Can. Conf. Electr. Comput. Eng. (CCECE), May 2015, pp. 57–62, doi: 10.1109/CCECE.2015.7129160.
34. T. S. Tran, D. T. Nguyen, and G. Fujita, ‘‘Islanding detection method based on injecting perturbation signal and rate of change of output power in DC grid-connected photovoltaic system,’’ Energies, vol. 11, no. 5, p. 1313, 2018, doi: 10.3390/en11051313.
35. T. Z. Bei, ‘‘Accurate active islanding detection method for grid-tied inverters in distributed generation,’’ IET Renew. Power Gener., vol. 11, no. 13, pp. 1633–1639, 2017, doi: 10.1049/iet-rpg.2017.0080.
36. L. A. C. Lopes and H. Sun, ‘‘Performance assessment of active frequency drifting islanding detection methods,’’ IEEE Trans. Energy Convers., vol. 21, no. 1, pp. 171–180, Mar. 2006, doi: 10.1109/TEC.2005.859981.
37. A. Yafaoui, B. Wu, and S. Kouro, ‘‘Improved active frequency drift antiislanding detection method for grid connected photovoltaic systems,’’ IEEE Trans. Power

Electron., vol. 27, no. 5, pp. 2367–2375, May 2012, doi: 10.1109/TPEL.2011.2171997.

38. B. Wen, D. Boroyevich, R. Burgos, Z. Shen, and P. Mattavelli, ‘‘Impedance-based analysis of active frequency drift islanding detection for grid-tied inverter system,’’ IEEE Trans. Ind. Appl., vol. 52, no. 1, pp. 332–341, Jan./Feb. 2016, doi: 10.1109/TIA.2015.2480847.
39. M. I. Chehardeh and E. M. Siavashi, ‘‘A novel hybrid islanding detection method for inverter-based DGs using SFS and ROCOF,’’ IEEE Trans. Power Del., vol. 32, no. 5, pp. 2162–2170, Oct. 2017.
40. C. L. Trujillo, D. Velasco, E. Figueres, and G. Garcerá, ‘‘Analysis of active islanding detection methods for grid-connected microinverters for renewable energy processing,’’ Appl. Energy, vol. 87, no. 11, pp. 3591–3605, Nov. 2010, doi: 10.1016/j.apenergy.2010.05.014.
41. H. Vahedi and M. Karrari, ‘‘Adaptive fuzzy Sandia frequency-shift method for islanding protection of inverter-based distributed generation,’’ IEEE Trans. Power Del., vol. 28, no. 1, pp. 84–92, Jan. 2013, doi: 10.1109/TPWRD.2012.2219628.
42. M. V. G. Reis, T. A. S. Barros, A. B. Moreira, P. S. Nascimento, F. E. Ruppert, and M. G. Villalva, ‘‘Analysis of the Sandia frequency shift (SFS) islanding detection method with a single-phase photovoltaic distributed generation system,’’ in Proc. IEEE PES Innov. Smart Grid Technol. Latin Amer. (ISGT LATAM), Oct. 2015, pp. 125–129, doi: 10.1109/ISGT-LA.2015.7381140.
43. M. El-Moubarak, M. Hassan, and A. Faza, ‘‘Performance of three islanding detection methods for grid-tied multi-inverters,’’ in Proc. IEEE 15th Int. Conf. Environ. Electr. Eng. (EEEIC), Jun. 2015, pp. 1999–2004, doi: 10.1109/EEEIC.2015.7165481.
44. B. Bahrani, H. Karimi, and R. Iravani, ‘‘Nondetection zone assessment of an active islanding detection method and its experimental evaluation,’’ IEEE Trans. Power Del., vol. 26, no. 2, pp. 517–525, Apr. 2011, doi: 10.1109/TPWRD.2009.2036016.
45. P. Li, Y. Sheng, L. Zhang, X. Yang, and Y. Zhao, ‘‘A novel active islanding detection method based on current-disturbing,’’ in Proc. Int. Conf. Electr. Mach. Syst., Nov. 2009, pp. 5–9, doi: 10.1109/ICEMS.2009.5382711.

46. H. H. Zeineldin, E. F. El-Saadany, and M. M. A. Salama, ‘‘Impact of DG interface control on islanding detection and nondetection zones,’’ IEEE Trans. Power Del., vol. 21, no. 3, pp. 1515–1523, Jul. 2006, doi: 10.1109/TPWRD.2005.858773.
47. F. Liu, Y. Kang, Y. Zhang, S. Duan, and X. Lin, ‘‘Improved SMS islanding detection method for grid-connected converters,’’ IET Renew. Power Gener., vol. 4, no. 1, pp. 36–42, Jan. 2010, doi: 10.1049/ietrpg.2009.0019.
48. S. Akhlaghi, A. Akhlaghi, and A. A. Ghadimi, ‘‘Performance analysis of the slip mode frequency shift islanding detection method under different inverter interface control strategies,’’ in Proc. IEEE Power Energy Conf. Illinois (PECI), Feb. 2016, pp. 1–7, doi: 10.1109/PECI.2016.7459250.
49. A. Emadi, H. Afrakhte, and J. Sadeh, ‘‘Fast active islanding detection method based on second harmonic drifting for inverter-based distributed generation,’’ IET Gener., Transmiss. Distrib., vol. 10, no. 14, pp. 3470–3480, 2016, doi: 10.1049/iet-gtd.2016.0089.
50. R. Haider, C. H. Kim, T. Ghanbari, S. B. A. Bukhari, M. Saeed uz Zaman, S. Baloch, and Y. S. Oh, ‘‘Passive islanding detection scheme based on autocorrelation function of modal current envelope for photovoltaic units,’’ IET Gener., Transmiss. Distrib., vol. 12, no. 3, pp. 726–736, Feb. 2018, doi: 10.1049/iet-gtd.2017.0823.
51. H. Abdi, A. Rostami, and N. Rezaei, ‘‘A novel passive islanding detection scheme for synchronous-type DG using load angle and mechanical power parameters,’’ Electr. Power Syst. Res., vol. 192, Mar. 2021, Art. no. 106968, doi: 10.1016/j.epsr.2020.106968.
52. X. Xie, C. Huang, and D. Li, ‘‘A new passive islanding detection approach considering the dynamic behavior of load in microgrid,’’ Int. J. Electr. Power Energy Syst., vol. 117, May 2020, Art. no. 105619, doi: 10.1016/j.ijepes.2019.105619.
53. X. Xie, W. Xu, C. Huang, and X. Fan, ‘‘New islanding detection method with adaptively threshold for microgrid,’’ Electr. Power Syst. Res., vol. 195, Jun. 2021, Art. no. 107167, doi: 10.1016/j.epsr.2021.107167.
54. B. K. Choudhury, S. Member, P. Jena, and S. Member, ‘‘Superimposed impedance based passive islanding detection scheme for DC microgrids,’’ IEEE

J. Emerg. Sel. Topics Power Electron., early access, Apr. 29, 2021, doi: 10.1109/JESTPE.2021.3076459.

55. A. G. Abd-Elkader, S. M. Saleh, and M. B. M. Eiteba, ‘‘A passive islanding detection strategy for multi-distributed generations,’’ Int. J. Electr. Power Energy Syst., vol. 99, pp. 146–155, Jul. 2018, doi: 10.1016/j.ijepes.2018.01.005.
56. P. P. Mishra and C. N. Bhende, ‘‘Islanding detection based on variational mode decomposition for inverter based distributed generation systems,’’ IFAC-PapersOnLine, vol. 52, no. 4, pp. 306–311, 2019, doi: 10.1016/j.ifacol.2019.08.216.
57. A. Rostami, J. Olamaei, and H. Abdi, ‘‘Islanding detection of synchronous DG based on inherent feature extracted from mechanical power,’’ Iranian J. Sci. Technol., Trans. Electr. Eng., vol. 43, no. 4, pp. 919–928, Dec. 2019, doi: 10.1007/s40998-019-00193-8.
58. A. Shahmohammadi and M. T. Ameli, ‘‘Proper sizing and placement of distributed power generation aids the intentional islanding process,’’ Electr. Power Syst. Res., vol. 106, pp. 73–85, Jan. 2014, doi: 10.1016/j.epsr.2013.08.005.
59. W. K. A. Najy, H. H. Zeineldin, A. H. K. Alaboudy, and W. L. Woon, ‘‘A Bayesian passive islanding detection method for inverter-based distributed generation using ESPRIT,’’ IEEE Trans. Power Del., vol. 26, no. 4, pp. 2687–2696, Oct. 2011, doi: 10.1109/TPWRD.2011.2159403.
60. K. Naraghipour, K. Ahmed, and C. Booth, ‘‘A comprehensive review of islanding detection methods for distribution systems,’’ in Proc. 9th Int. Conf. Renew. Energy Res. Appl. (ICRERA), Sep. 2020, pp. 428–433, doi: 10.1109/ICRERA49962.2020.9242850.
61. D. Motter and J. C. M. Vieira, ‘‘Improving the islanding detection performance of passive protection by using the undervoltage block function,’’ Electr. Power Syst. Res., vol. 184, Jul. 2020, Art. no. 106293, doi: 10.1016/j.epsr.2020.106293.
62. P. Gupta, R. S. Bhatia, and D. K. Jain, ‘‘Active ROCOF relay for Islanding detection,’’ IEEE Trans. Power Del., vol. 32, no. 1, pp. 420–429, Feb. 2017, doi: 10.1109/TPWRD.2016.2540723.
63. M. R. Alam, M. T. A. Begum, and K. M. Muttaqi, ‘‘Assessing the performance of ROCOF relay for anti-islanding protection of distributed generation under

subcritical region of power imbalance,'' IEEE Trans. Ind. Appl., vol. 55, no. 5, pp. 5395–5405, Sep. 2019, doi: 10.1109/TIA.2019.2927667.

64. C. R. Reddy and K. H. Reddy, ''Islanding detection method for inverter based distributed generation based on combined changes of ROCOAP and ROCORP,'' Int. J. Pure Appl. Math., vol. 117, no. 19, pp. 433–440, 2017. [Online]. Available: http://www.ijpam.eu.
65. D. Salles, W. Freitas, J. C. M. Vieira, and B. Venkatesh, ''A practical method for nondetection zone estimation of passive anti-islanding schemes applied to synchronous distributed generators,'' IEEE Trans. Power Del., vol. 30, no. 5, pp. 2066–2076, Oct. 2015, doi: 10.1109/TPWRD.2014.2360299.
66. W. Freitas, W. Xu, C. M. Affonso, and Z. Huang, ''Comparative analysis between ROCOF and vector surge relays for distributed generation applications,'' IEEE Trans. Power Del., vol. 20, no. 2, pp. 1315–1324, Apr. 2005, doi: 10.1109/TPWRD.2004.834869.
67. S. Khichar and M. Lalwani, ''An analytical survey of the islanding detection techniques of distributed generation systems,'' Technol. Econ. Smart Grids Sustain. Energy, vol. 3, no. 1, pp. 1–10, Dec. 2018, doi: 10.1007/s40866-018-0041-1.
68. G. Marchesan, M. R. Muraro, G. Cardoso, L. Mariotto, and A. P. de Morais, ''Passive method for distributed-generation island detection based on oscillation frequency,'' IEEE Trans. Power Del., vol. 31, no. 1, pp. 138–146, Feb. 2016, doi: 10.1109/TPWRD. 2015.2438251.
69. G. Wang, F. Gao, and J. Liu, ''A hybrid islanding detection method combining VU/THD and BRPV,'' in Proc. IEEE Energy Convers. Congr. Expo. (ECCE), Sep. 2018, pp. 3682–3687, doi: 10.1109/ECCE.2018.8557792.
70. S.-I. Jang and K.-H. Kim, ''An islanding detection method for distributed generations using voltage unbalance and total harmonic distortion of current,'' IEEE Trans. Power Del., vol. 19, no. 2, pp. 745–752, Apr. 2004, doi: 10.1109/TPWRD.2003.822964.
71. A. Llaria, O. Curea, J. Jiménez, and H. Camblong, ''Survey on microgrids: Unplanned islanding and related inverter control techniques,'' Renew. Energy, vol. 36, no. 8, pp. 2052–2061, Aug. 2011, doi: 10.1016/j.renene.2011.01.010.
72. I. Pvps, ''Evaluation of islanding detection methods for photovoltaic utility-interactive power systems,'' Tech. Rep. IEA PVPS T5-09, 2002.

73. D. Velasco, C. L. Trujillo, G. Garcerá, and E. Figueres, ‘‘Review of anti-islanding techniques in distributed generators,’’ Renew. Sustain. Energy Rev., vol. 14, no. 6, pp. 1608–1614, Aug. 2010, doi: 10.1016/j.rser.2010.02.011.
74. S. D. Kermany, M. Joorabian, S. Deilami, and M. A. S. Masoum, ‘‘Hybrid islanding detection in microgrid with multiple connection points to smart grids using fuzzy-neural network,’’ IEEE Trans. Power Syst., vol. 32, no. 4, pp. 2640–2651, Jul. 2017, doi: 10.1109/TPWRS.2016. 2617344.
75. M. Seyedi, S. A. Taher, B. Ganji, and J. Guerrero, ‘‘A hybrid islanding detection method based on the rates of changes in voltage and active power for the multi-inverter systems,’’ IEEE Trans. Smart Grid, vol. 12, no. 4, pp. 2800–2811, Jul. 2021, doi: 10.1109/TSG.2021.3061567.
76. K. Narayanan, S. A. Siddiqui, and M. Fozdar, ‘‘Hybrid islanding detection method and priority-based load shedding for distribution networks in the presence of DG units,’’ IET Gener., Transmiss. Distrib., vol. 11, no. 3, pp. 586–595, 2017, doi: 10.1049/iet-gtd.2016.0437.
77. V. Menon and M. H. Nehrir, ‘‘A hybrid islanding detection technique using voltage unbalance and frequency set point,’’ IEEE Trans. Power Syst., vol. 22, no. 1, pp. 442–448, Feb. 2007, doi: 10.1109/TPWRS.2006.887892.
78. S. Padmanaban, N. Priyadarshi, M. Sagar Bhaskar, J. B. Holm-Nielsen, V. K. Ramachandaramurthy, and E. Hossain, ‘‘A hybrid ANFIS-ABC based MPPT controller for PV system with anti-islanding grid protection: Experimental realization,’’ IEEE Access, vol. 7, pp. 103377–103389, 2019, doi: 10.1109/ACCESS.2019.2931547.
79. S. C. Paiva, R. L. D. A. Ribeiro, D. K. Alves, F. B. Costa, and T. D. O. A. Rocha, ‘‘A wavelet-based hybrid islanding detection system applied for distributed generators interconnected to AC microgrids,’’ Int. J. Electr. Power Energy Syst., vol. 121, Oct. 2020, Art. no. 106032, doi: 10.1016/j.ijepes.2020.106032.
80. G. Wang and S. University, ‘‘Design consideration and performance analysis of a hybrid islanding detection method combining voltage unbalance/total harmonic distortion and bilateral reactive power variation,’’ CPSS Trans. Power Electron. Appl., vol. 5, no. 1, pp. 86–100, Mar. 2020, doi: 10.24295/cpsstpea.2020.00008.
81. M. R. Alam, K. M. Muttaqi, and A. Bouzerdoum, ‘‘An approach for assessing the effectiveness of multiple-feature-based SVM method for islanding detection

of distributed generation,'' IEEE Trans. Ind. Appl., vol. 50, no. 4, pp. 2844–2852, Jul./Aug. 2014, doi: 10.1109/TIA.2014.2300135.

82. S. R. Samantaray and S. Kar, ''Data-mining-based intelligent antiislanding protection relay for distributed generations,'' IET Gener., Transmiss. Distrib., vol. 8, no. 4, pp. 629–639, 2014, doi: 10.1049/ietgtd.2013.0494.
83. A. Taheri Kolli and N. Ghaffarzadeh, ''A novel phaselet-based approach for islanding detection in inverter-based distributed generation systems,'' Electr. Power Syst. Res., vol. 182, May 2020, Art. no. 106226, doi: 10.1016/j.epsr.2020.106226.
84. R. Bakhshi-Jafarabadi, J. Sadeh, J. D. J. Chavez, and M. Popov, ''Two-level islanding detection method for grid-connected photovoltaic system-based microgrid with small non-detection zone,'' IEEE Trans. Smart Grid, vol. 12, no. 2, pp. 1063–1072, Mar. 2021, doi: 10.1109/TSG.2020.3035126.
85. J. Merino, P. Mendoza-Araya, G. Venkataramanan, and M. Baysal, ''Islanding detection in microgrids using harmonic signatures,'' IEEE Trans. Power Del., vol. 30, no. 5, pp. 2102–2109, Oct. 2015, doi: 10.1109/TPWRD.2014.2383412.
86. U. Markovic, D. Chrysostomou, P. Aristidou, and G. Hug, ''Impact of inverter-based generation on islanding detection schemes in distribution networks,'' Electr. Power Syst. Res., vol. 190, Jan. 2021, Art. no. 106610, doi: 10.1016/j.epsr.2020.106610.
87. B. Matic-cuka and M. Kezunovic, ''Islanding detection for inverterbased distributed generation using support vector machine method,'' IEEE Trans. Smart Grid, vol. 5, no. 6, pp. 2676–2686, Nov. 2014, doi: 10.1109/TSG.2014.2338736.
88. H. Samet, F. Hashemi, and T. Ghanbari, ''Islanding detection method for inverter-based distributed generation with negligible non-detection zone using energy of rate of change of voltage phase angle,'' IET Gener., Transmiss. Distrib., vol. 9, no. 15, pp. 2337–2350, 2015, doi: 10.1049/iet-gtd. 2015.0638.
89. R. S. Kunte and W. Gao, ''Comparison and review of islanding detection techniques for distributed energy resources,'' in Proc. 40th North Amer. Power Symp., Sep. 2008, pp. 1–8, doi: 10.1109/NAPS.2008. 5307381.
90. D. Velasco, C'. Trujillo, G. Garcer'a and E. Figueres, "An active antiislanding method based on phase-PLL perturbation", *IEEE Transactions on Power Electronics*, vol. 26, no. 4, pp. 1056-1066, Oct. 2010.

91. R. A. Mastromauro, "Grid Synchronization and Islanding Detection Methods for Single-Stage Photovoltaic Systems", *Energies*, vol. 13, pp. 3382, Jan. 2020.
92. H. Karimi, A. Yazdani and R. Iravani, "Negative-sequence current injection for fast islanding detection of a distributed resource unit", *IEEE Transaction on power electronics*, vol. 23, no. 1, pp. 298-307, Jan. 2008.
93. N. Chothani and I. Desai, "Fourier Transform and Probabilistic Neural Network based Fault Detection in Distribution System Containing DGs," 2021 Innovations in Power and Advanced Computing Technologies (i-PACT), Kuala Lumpur, Malaysia, 2021, pp. 1-5, doi: 10.1109/i-PACT52855.2021.9696718.
94. B. Matic-Cuka and M. Kezunovic, "Islanding Detection for Inverter-Based Distributed Generation Using Support Vector Machine Method," in IEEE Transactions on Smart Grid, vol. 5, no. 6, pp. 2676-2686, Nov. 2014, doi: 10.1109/TSG.2014.2338736.
95. H. R. Baghaee, D. Mlakić, S. Nikolovski and T. Dragicević, "Support Vector Machine-Based Islanding and Grid Fault Detection in Active Distribution Networks," in IEEE Journal of Emerging and Selected Topics in Power Electronics, vol. 8, no. 3, pp. 2385-2403, Sept. 2020, doi: 10.1109/JESTPE.2019.2916621.
96. F. Záplata and M. Kasal, "Using the Goertzel algorithm as a filter," 2014 24th International Conference Radioelektronika, Bratislava, Slovakia, 2014, pp. 1-3, doi: 10.1109/Radioelek.2014.6828441.
97. T. Guo, T. Zhang, E. Lim, M. López-Benítez, F. Ma and L. Yu, "A Review of Wavelet Analysis and Its Applications: Challenges and Opportunities," in IEEE Access, vol. 10, pp. 58869-58903, 2022, doi: 10.1109/ACCESS.2022.3179517.
98. J. -H. Kim, J. -G. Kim, Y. -H. Ji, Y. -C. Jung and C. -Y. Won, "An Islanding Detection Method for a Grid-Connected System Based on the Goertzel Algorithm," in IEEE Transactions on Power Electronics, vol. 26, no. 4, pp. 1049-1055, April 2011, doi: 10.1109/TPEL.2011.2107751.
99. S. R. Samantaray, K. El-Arroudi, G. Joós and I. Kamwa, "A Fuzzy Rule-Based Approach for Islanding Detection in Distributed Generation," in IEEE Transactions on Power Delivery, vol. 25, no. 3, pp. 1427-1433, July 2010, doi: 10.1109/TPWRD.2010.2042625.

100. S. Swetha and V. Verma, "Autonomous Active Grid islanding and DGs outage detection in a $\mu \mathrm{G}$ utilizing Goertzel Algorithm in collaboration with Fuzzy Inferencing System," 2023 IEEE IAS Global Conference on Renewable Energy and Hydrogen Technologies (GlobConHT), Male, Maldives, 2023, pp. 1-6, doi: 10.1109/GlobConHT56829.2023.10087768.

PUBLICATIONS

1. **PUBLISHED:** S. Swetha and V. Verma, "Autonomous Active Grid islanding and DGs outage detection in a $\mu \mathrm{G}$ utilizing Goertzel Algorithm in collaboration with Fuzzy Inferencing System," 2023 IEEE IAS Global Conference on Renewable Energy and Hydrogen Technologies (GlobConHT), Male, Maldives, 2023, pp. 1-6, doi: 10.1109/GlobConHT56829.2023.10087768.